Reverse Engineering a Model for T-Cell Vaccination

Lee A. Segel
Eva Jäger

SFI WORKING PAPER: 1993-09-058

SANTA FE INSTITUTE

REVERSE ENGINEERING A MODEL FOR T-CELL VACCINATION

• LEE A. SEGEL and EVA JÄGER
Department of Applied Mathematics & Computer Science
Weizmann Institute of Science, Rehovot 76100, Israel
[E-mail: masegel@weizmann.weizmann.ac.il]
and on leave during 1992-3 academic year at
Center for Nonlinear Studies, and Theoretical Biology and Biophysics Group
Los Alamos National Laboratory, Los Alamos, NM 87545, U.S.A.
[E-mail: las@life.lanl.gov]

A class of minimal models is constructed that can exhibit several salient phenomena associated with T-cell inoculations that prevent and cure auto-immune disease. The models consist of differential equations for the magnitude of two populations, the effectors E (which cause the disease), and an interacting regulator population R. In these models, normality, vaccination, and disease are identified with stable steady states of the differential equations. Thereby accommodated by the models are a variety of findings such as the induction of vaccination or disease, depending on the size of the effector inoculant. Features such as spontaneous acquisition of disease and spontaneous cure require that the models be expanded to permit slow variation of their coefficients and hence slow shifts in the number of steady states. Other extensions of the basic models permit them to be relevant to vaccination by killed cells or by antigen, or to the interaction of a larger number of cell types. The discussion includes an indication of how the highly simplified approach taken here can serve as a first step in a modelling program that takes increasing cognizance of relevant aspects of known immunological physiology. Even at its present stage, the theory leads to several suggestions for experiments.

1. Introduction. Reverse engineering, a legal activity, is "the copying of all or part of a chip for the purpose of analyzing its layout" (Fauch, 1993). The attitude that we take here is somewhat similar. We describe some of the major phenomenology associated with T-cell vaccination. We then attempt to construct a minimal model, in the form of differential equations, that will reproduce this phenomenology. Insofar as possible, we remain neutral as to the form that this simple model of nature's "product" will take, letting the phenomenology be our guide. A variety of models can, of course, describe a given set of facts. We find, however, that requirements of internal mathematical consistency considerably constrain the nature of the models.

Because of this, our resulting models are more than merely descriptive and have a life of their own.

We construct a class of mathematical models, containing just two cell populations, that can describe several salient observed features of T-cell vaccination in suitable strains of mice and rats: notably, whereas sufficiently high dose injections of virulent autoimmune T-cells induce disease, relatively low doses generate resistance to a subsequent high dose. In some instances, cure can be obtained. In the course of our investigation, new possibilities are revealed, such as "over cure" (suitable doses can return a diseased organism to the normal state, not the vaccinated state). Modification of our basic models allows consideration of more cell populations as well as of perturbations via antigens or killed cells. Other modifications yield the observed phenomena of spontaneous disease and spontaneous cure. In concluding, we discuss several possible experiments that are suggested by the theory.

2. The Phenomenology of T-cell Vaccination. We now provide a general description of major phenomena connected with T-cell vaccination. For definiteness, we concentrate, although not exclusively, on the case of experimental autoimmune encephalomyelitis (EAE), an animal model of multiple sclerosis.

In the course of experiments concerning T-cell vaccination, different states of an animal are recognized. An animal is termed *normal* when it is healthy but has had no experience with the disease and therefore is susceptible to it. A *vaccinated* animal is healthy and furthermore is resistant to manipulations that bring about the onset of disease in a normal animal. Finally there is the *diseased* state. Since we are dealing with autoimmune diseases, it is reasonable to suppose that the effector cell population, whose presence by definition causes autoimmune disease, is respectively low and high in the normal and diseased states.

During investigations of T-cell vaccination in EAE, it has been found that disease can be induced in a normal animal by injecting it with a large quantity of live effector cells that have been suitably activated, for example by incubation with antigen-presenting cells and a suitable antigen (Naparstek et al., 1983). Injection of a considerably smaller quantity of such cells induces vaccination (Cohen, 1986; Beraud et al., 1989). T-cell vaccination is carried out not only with low doses of virulent cells but also with larger doses of such cells that have been killed and

treated in various ways, such as by irradiation and chemical cross-linkers (Ben Nun, Wakerle, and Cohen, 1981; Lider et al., 1986; Alborán et al., 1992).

When we describe cell populations as small, medium, and large, we mean these terms in a very rough comparative sense. Furthermore in our simple models, the magnitude of a variable that represents a population includes in it both the actual numbers of the cells in question and their degree of "activity". For example, in the crude type of modelling that we are doing here, we cannot distinguish between a relatively small population of fully activated cells and a larger population of relatively ineffective cells.

A major property of T-cell vaccination with killed cells is that not only is it capable of inducing protection against a disease but it may also bring about a cure of disease. When cure occurs, if a diseased animal is subjected to a suitable dose of effector cells, then the symptoms of disease disappear and the animal usually enters a vaccinated state. Mice and rats induced to exhibit EAE spontaneously return to health after a few days (sometimes with relapses). Strictly speaking, therefore, one cannot speak of a treatment that induces cure – although inoculations of selected T cell receptors have greatly speeded up spontaneous recovery (Offner, Hashim and Vandenbark, 1991). On the other hand, for persistent diseases such as adjuvant arthritis (Lider et al., 1986) and spontaneous autoimmune diabetes (Elias et al., 1991), inoculation of killed T cells can bring about cure.

The various phenomena associated with T-cell vaccination are summarized in Table 1. The table contains a column giving a mnemonic for the various manipulations. For example, in the third line the letters NlD mean that a *N*ormal state, by virtue of a *l*arge perturbation of effectors, is transformed into a *D*iseased state. These various triplets of letters will be useful in labelling phenomena on diagrams that follow. Note that the properties NsN and DsD are listed for completeness. In spite of the fact that no specific evidence is known, it seems almost inevitable, for example, that although a suitable inoculant of cells can induce vaccination, too small an inoculant will have no effect. Note also that, although the second line of Table 1 indicates that a medium amount of either live or killed cells can induce vaccination, in fact, a relatively large number of killed cells is required. Since a killed cell is presumably less efficacious than a live cell, the differing number of cells covered by the word "medium" is consistent with the remark made above that

both number and activity are included in our model characterizations of population magnitudes.

The phenomena in Table 1 are what we wish our model to reproduce. At first we shall assume that all the phenomena have been generated by suitable doses of live cells. In fact (as indicated in the table), it remains an open question as to whether live cells can effect a cure. In any case, later we modify the model so that it is appropriate for injections of killed cells.

3. One Variable: The Simplest Possible Model. The simplest possible model would involve just a single cell population, the *effectors* E. The qualitative behavior of such a model is summarized in the "phase line" diagram given in Fig. 1. There we see three steady states, N, V, and D, corresponding to the normal, vaccinated, and diseased states of the experimental animal. Embodied here is the major *assumption* that the *normal, vaccinated and diseased states of the organism correspond to steady states* in the dynamical system that constitutes our mathematical model.

The objection can be raised that in a real animal it may not be true that a steady state is an appropriate representation for disease. The varying environmental influences to which an animal is subject, or the aging of the animal, can continually modify its state of health or disease. Disease can be transient, either because the immune system eventually cures it, or because exacerbating disease inexorably leads to the death of an animal. These are valid objections, which will be dealt with further later. For the present, we remark that if the diseased state persists for a significant period of time without major alterations, then as a first approximation and for a limited period it is reasonable to regard disease (as well as normalcy and vaccination) as steady states of our basic model. With respect to disease, this assumption gains further credence if it is kept in mind that the effector population may remain relatively constant over a fairly long time, but the clinical state may continually worsen owing to accumulated damage.

Returning to Fig. 1, we note points S_1 and S_2 that respectively divide regions of normality from those leading to vaccination, and regions of vaccination from those leading to disease. In particular, if one begins with an effector population that is smaller than S_1, as time develops (as shown by the arrows) the effector cell population decreases to the steady state N. (Note that, although it is not essential, we have chosen the normal state to be one that is devoid of effector cells.) By

contrast, a population of effector cells that is slightly above the value S_1 will grow toward the vaccinated steady state V. (Thus the interval between S_1 and S_2 is called the *domain of attraction of* V.) A population of effector cells that is precisely at the value S_1 in principle hovers precisely at this value, unable to "decide" whether to approach N or V. Thus the value $E = S_1$ is a steady state, but an unstable one: the slightest perturbation induces E either to decrease to N or to increase to V.

A differential equation for $E(t)$ whose qualitative behavior is correctly described in Fig. 1, is

$$\frac{dE}{dt} = E(E - S_1)(V - E)(S_2 - E)(D - E) \quad . \qquad (3.1)$$

In this equation, the constants S_1, V, S_2, and D correspond to the different levels of effector cell that were singled out in Fig. 1.

The simple model whose behavior is diagrammed in Fig. 1 is capable of reproducing four of the six behaviors listed in Table 1. For example we note in Fig. 1 that small, medium, and large perturbations of the normal state lead respectively to normality, vaccination, and disease. However, the two most important properties of T-cell vaccination are not reproduced by this simple model. Contrary to observation, a perturbation that is of sufficient magnitude to induce disease when applied to a normal organism also induces disease when applied to a vaccinated organism. According to the model of Fig. 1, only smaller perturbations to the vaccinated state will leave this state intact. Moreover, the model of Fig. 1 offers no possibility of cure. Any addition of effector cells to the diseased state will bring about reversion to disease, not vaccination.

Strictly speaking, it is possible to modify (3.1) by adding another linear factor in order to obtain a model that exhibits all six transitions of Table 1. This revised model is quite unnatural, however, in that as the effector population increases above the diseased state, one must postulate the existence of a second vaccinated state. There seems no biological justification for such a hypothesis. Moreover, biological credibility requires some type of separate representation of the factors regulating the effector population E, and being regulated by it. We thus supplement the equation for E with a second equation for an interacting regulatory population R.

4. Two Variables: The Simplest Successful Model. Fig. 2 is an analog of Fig. 1 showing that a two-variable model is in principle capable of reproducing all of

the qualitative behavior described in Table 1. Fig. 2 contains a schematic diagram that exhibits the behavior of two populations, the original effector cells E, and a second, *regulating*, population that we term R cells. At present we do not wish to commit ourselves as to the expected behavior of the R cell population, for we wish this to evolve naturally from the requirements that we put on the model. All we assume *a priori* is that the proliferation rate of the R population is affected by a population of effector cells E that in turn is driven by the self-antigen.

In Fig. 2, the three major steady states are once again represented – normal, vaccinated, and diseased – with respectively larger populations of effector cells E. Anticipating future findings, we positioned the vaccinated state so that it is associated with a relatively high value of R although at the moment this is not a matter of importance. What is crucial is the postulated existence of *separatrix* lines that separate the domains of attraction of the three steady states. For example, in Fig. 2 initial conditions to the left of separatrix A result in solutions that tend to the normal state N; initial conditions to the right of A (but not too far to the right) result in the development of R and E populations in such a way that the vaccinated state V is ultimately attained.

One sees from examination of Fig. 2 that indeed all the various transformations of Table 1 can be accommodated. In particular, the transformation VlV appears, corresponding to the situation in which a large number of effectors are added to the vaccinated state but yet the system returns to the vaccinated state. This is in contrast to the situation in which a large number of effector cells are added to the normal state and disease develops (NlD). We also note on the diagram that a sufficiently large addition of effector cells to the diseased state results in a return to vaccination (DlV), and hence cure.

4.1. The Mathematical Framework. The general form of a two-variable model is

$$\frac{dE}{dt} = f(E,R), \qquad \frac{dR}{dt} = g(E,R) \ . \tag{4.1a,b}$$

We must choose the functions f and g so that the qualitative behavior depicted in Fig. 2 will be attained. In making these choices, we cannot let imagination run unchecked. There are a number of constraints (well known to mathematicians) that flow from the very existence of equations of the general form of (4.1a,b). For example, at all points E and R where the function g vanishes, we note that $dR/dt =$

0. This means that trajectories in the (E, R) *phase plane* must be horizontal at the points in question. Similarly, at all points where f vanishes, trajectories must be vertical. These requirements on horizontally and verticality are responsible for the standard terms *horizontal* and *vertical nullclines* for curves where g and f respectively vanish.

It follows from (4.1) that at any point (E, R) that is such that both $f = 0$ and $g = 0$, a steady state must exist. That is, steady states exist at points where vertical and horizontal nullclines intersect, and only at such points. These well known facts concerning differential equations are illustrated in Fig. 3. Another constraint on the models is that all cell population variables must remain positive, as a negative value of a cell population makes no sense.

Recall from Fig. 1 that the separating points that divide the domains of attraction of the three steady states N, V, D were in fact unstable steady state points of the equation. The two-dimensional version of this phenomenon, illustrated in Fig. 4A, is that each separatrix contains an unsteady state point S of the saddle point type (see inset to Fig. 4A). (Unstable limit cycles can also form separatrices, but we shall not pursue this option.)

We now specialize equations (4.1) so that they take the form

$$\frac{dE}{dt} = EP_E(E, R) \quad , \quad \frac{dR}{dt} = RP_R(E, R) \quad . \qquad (4.2a, b)$$

Here the functions P_E and P_R are effective proliferation rates. If for example P_E is a positive constant, then the effector cell population grows exponentially. As it is, both P_E and P_R can in principle be either positive or negative, depending upon the values of E and R. Note that P_E and P_R are generally a combination of several not-clearly-identified processes, hence their designation as "effective proliferation rates".

In writing equations in the form of (4.2) we have assumed that there are no source terms for the cells E and R that are independent of the E and R population levels. In particular, this means that for the moment we are regarding as negligible the steady flux of T-cells from the thymus. Note, as illustrated in Fig. 4B, that the assumption (4.2) means that the vertical and horizontal axes are respectively vertical and horizontal nullclines. As it is the intersection of vertical and horizontal nullclines, the origin is a steady state, but it will be unstable in our model.

Fig. 4B schematically sums up further requirements. Each of the five steady states N, V, D, S_1 and S_2 is indicated to be at the intersection of a vertical and a horizontal nullcline. S_1 and S_2 are saddle points with the separatrices (ingoing arrows) indicated. Given that N has a low effector population, it is reasonable to locate it on the R axis ($E = 0$). Note that the separatrix that rises above the point S_2 must fall back below it, in order to produce the mound-like domain of attraction of the disease state that is shown in Fig. 2 to be essential for the DIV trajectory. This separatrix, as shown, possesses a maximum, which must lie on a horizontal nullcline.

4.2. Some Specific Examples. One is now faced with the task of constructing a pair of differential equations of the form (4.2) that possess all the desired properties. An example of such a system is

$$\begin{aligned} \frac{dE}{dt} &= E(R+E-2)(-R-E+10) \ , \\ \frac{dR}{dt} &= R(-R+E+1)(-R+E-4)(-R+E-6) \ . \end{aligned} \qquad (4.3a,b)$$

The corresponding phase plane is diagrammed in Fig. 5. In particular, Fig. 5 shows the vertical and horizontal nullclines (light lines), with the directions of trajectories also indicated. In Fig. 5 shading shows the domain of attraction of the stable steady state N (normal) while stippling indicates the domain of attraction of the disease state D. The domain of attraction of the vaccinated state V is thus the unshaded and unstippled area. [The separatrices are computed by the well known expedient of starting at the unstable steady states and "running time backward", which amounts to preceding the righthand sides of (4.3) by negative signs.] It can be verified that the various qualitative trajectories of Fig. 4B are present in Fig. 5, so that the system (4.3) indeed fulfills the requirements that we have put forward for our model.

A further constraint on all our models is illustrated in Fig. 5. For example, on the vertical nullcline labeled with an asterisk we note that the vertical arrows switch from downward to upward, to downward and again upward, as the three different slanting horizontal nullclines are crossed. This is once again a well known property that is normally exhibited in a phase plane diagram.

The model given by (4.3) is especially simple in that all of the nullclines are straight lines. The equations of (4.3) certainly are not a unique solution to our problem of constructing a mathematical model with appropriate phase plane behavior. There is considerable latitude in the coefficients of the model, but not by any means complete latitude. For example, by rotating and translating the vertical nullcline that is labelled with an asterisk once can remove some or all of the intersections V, S_2, D, and S_3.

Another possible model is given by

$$\begin{aligned} \frac{dE}{dt} &= E(R+E-2)(-R-0.2E+32) \ , \\ \frac{dR}{dt} &= R(-R+E+0.4)(0.5R+0.5E^2-6E+16) \ . \end{aligned} \tag{4.4a,b}$$

The phase plane diagram for this model is given in Fig. 6. The rightmost pair of straight slanting horizontal nullclines in Fig. 5 is now transformed into the single parabolic horizontal nullcline of Fig. 6. Nonetheless the required qualitative properties of Fig. 4B are preserved.

Further evidence of the extent of flexibility in constructing a mathematical model is demonstrated in Fig. 7 and the accompanying equations of a third alternative model

$$\begin{aligned} \frac{dE}{dt} &= E(R+E-2)(-R-0.2E+2.5) \ , \\ \frac{dR}{dt} &= R(-R+0.02E^3-\frac{1}{3}E^2+1.3E+1) \ . \end{aligned} \tag{4.5a,b}$$

We note that in Fig. 7 that the three slanting horizontal nullclines of Fig. 5 have been replaced by a single N shaped horizontal nullcline. There is a corresponding replacement of the three linear factors in (4.3b) by a single cubic factor in (4.5b).

In a final example, the pair of slanting lines that have served as vertical nullclines is replaced by a single, humped curve:

$$\begin{aligned} \frac{dE}{dt} &= 0.01+E\left(3.5-0.5R+\frac{100E^2}{25+E^4}\right) \ , \\ \frac{dR}{dt} &= 0.01+R(-0.1R+0.02E^3-0.33E^2+1.3E+1) \ . \end{aligned} \tag{4.6a,b}$$

In addition, the form (4.2) has been generalized to permit the inclusion of constant source terms. The corresponding phase plane is provided in Fig. 8. Note that,

in contrast to the earlier examples (4.3)-(4.5), the coordinate axes are no longer nullclines of (4.6). Concomitantly, three unnecessary (but not "harmful") unstable steady states have disappeared, namely O, U, and S_3. It can be seen once again that the new phase plane diagram of Fig. 8 is completely consistent with the various qualitative trajectories indicated in Fig. 4B.

The systems (4.3)-(4.6) all provide examples of specific models that satisfy the qualitative requirements illustrated in Fig. 4B. The choice of specific models is broad, but nonetheless one has a feeling that "all these models must be essentially the same". This matter is explored in Appendix A. One point is worth noting here. It is unbiological that the proliferation rate in (4.6b) increases without bound as E increases. This need not be worrisome as only a finite range of E will be of interest to us. But the problem can also be solved once and for all by dividing the right side of (4.6b) by a suitable function, for example, $0.01(1+E^3)$. The relevant qualitative behavior of the model is unaffected (not shown), and now the proliferation rate approaches a constant as $E \to \infty$.

We now present graphs of the development of the effector (E) and regulatory (R) cell populations as a function of the time t. Such graphs would normally be plotted in recording results of experiment. They reveal qualitative features of response kinetics.

4.3. Further Examination of Model Properties. Fig. 9 shows the development with time of various different phenomena characteristic of T-cell vaccination (compare Table 1). The system (4.5) has been used for these numerical calculations. We observe from this point of view the fact that small, medium, and large additions of effector cells to the normal state result respectively in return to normalcy, vaccination, or disease. Note from Fig. 9C that the approach to the diseased state is oscillatory.

Fig. 10A depicts the result of adding the same number of effector cells as was added to the normal state in Fig. 9C. As shown, when this number of cells is added to the vaccinated state, there is no disease but rather vaccination. Fig. 10B shows that addition of a small number of effectors to the diseased state results in an oscillatory return to disease. Fig. 10C, by contrast, shows that a larger perturbation of the diseased state leads to cure, via a transition to the vaccinated state. Note that the large number of effectors is rapidly suppressed by an increase in the regulating R

cell population. As we will see shortly, the R population does not always act to suppress the effector population, but in the population ranges that are relevant in Fig. 10C, suppression occurs.

We have demonstrated that suitable assumptions concerning the dependence of proliferation rates P_E and P_R on E and R will result in appropriate behavior of our two-variable model. What, in fact, is the assumed type of dependence of the proliferation rates? This can be seen in Figs. 11 and 12. Fig. 11 deals with the effector proliferation rate P_E. We note from Fig. 11A that P_E varies smoothly, with some positive values (growth) and some negative values (decay). For clarity, Fig. 11B depicts just the positive part of P_E while Fig. 11C shows the portion of the E, R plane wherein P_E is positive. Corresponding diagrams for the regulator cell's proliferation rate P_R are given in Fig. 12. The behavior here is somewhat more exotic but does not seem unreasonable.

In general, what is decisive about the proliferation rates is their sign, not their magnitude. As can be checked by comparing Figs. 11C and 12C with Fig. 6, the proliferation rates change sign when the nullclines are traversed. As we have seen, the intersections of the nullclines set the number and location of the steady state points and, therefore, play a dominant role in determining the qualitative behavior of the solutions.

The intersections of the nullclines are important, not the individual nullcline positions in isolation. In biological terms, it is the network that matters, not the individual population behaviors. Consider, for example, some changes that shrink the parabolic region in Fig. 12C where the regulator's proliferation rate P_R is positive. Up to a point, changes of this nature just slightly alter the reproductive behavior of the regulators. But suppose that the parabolic region were to shrink so much that it entirely overlapped with the shaded region in Fig. 11C, where P_E is positive. Then the intersections S_2 and D in Fig. 6 would disappear. The regulator-effector interaction is now of such a nature that no disease state exists. A profound alteration of network behavior suddenly flows from an insignificant-seeming modification in the proliferative behavior of a single cell population.

Under most circumstances, it makes little difference how positive or negative proliferation rates are. Such quantitative changes merely alter the speed at which things happen, not what happens. In the phase plane, these changes modify the

location of separatrices, without in general leading to qualitative behavioral consequences. But there are important exceptions, exemplified by the required mound-like nature of the separatrix associated with the possibility of cure. [See the the discussion in the paragraph preceding (4.3b).] According to our models, the magnitudes of the proliferation rates, not just their signs, can make all the difference between whether or not vaccination can induce cure. An analogous statement holds for the phenomenon of "over cure", to be discussed below.

5. Expanding the Model. The two-variable model can serve as the basis for making our model more comprehensive by including further cell populations that have been deemed active in T-cell vaccination. As a first illustration of the type of model expansion that can be made, let us consider two additional populations, a class of helper cells (H) and of suppressor cells (S). These additional populations will always be assumed to increase and decrease the proliferation rates of E and R, respectively. Our expanded model begins to be reminiscent of the five population automaton model of Cohen and Atlan (1989). Detailed comparison with assumptions of Cohen and Atlan, or others, is inappropriate since the discussion of this section is meant to illustrate in general terms how our two-variable model can serve as the core of more complex and realistic models. We wish to counter the natural feeling that the complexity of immune interactions cannot possibly be usefully represented in just two differential equations.

In our new model the proliferation rates P_R, P_E of (4.2) will depend not only on R and E but also on H and S. Moreover, two new equations are required.

$$\frac{dH}{dt} = P_H(R,E,H,S) \quad , \quad \frac{dS}{dt} = P_S(R,E,H,S) \quad . \tag{5.1}$$

In order to link our new model with the original model (4.2), we will temporarily make the assumption that, in comparison to R and E, the helper and suppressor populations H and S respond rapidly to environmental changes. (By "environmental changes" we mean changes in cytokine concentrations, or perhaps changes in concentrations of cells that are in contact with H and S cells, as reflected in the levels of R, E, H, and S.) The relatively rapid change of H and S means that we can make the quasi-steady state assumption (QSSA) that is common in enzyme kinetics (see Segel and Slemrod, 1989). By this assumption

$$P_H(R,E,H,S) = 0 \quad , \qquad P_S(R,E,H,S) = 0 \quad . \tag{5.2a,b}$$

According to (5.2) the cell populations H and S are at equilibrium with the present values of population levels R and E. Eqs. (5.2a) and (5.2b) can in general be solved for H and S as functions of R and E:

$$H = H(R,E) \ , \qquad S = S(R,E) \ . \tag{5.2c,d}$$

These solutions in turn provide the quasi-steady state values of helper and suppressor population levels that are appropriate to the present values of the E and R population variables. However, E and R slowly change with time, with consequent slow changes in H and S.

Knowing H and S in terms of R and E, we can regard the proliferation rates P_E and P_R not as functions of the four variables R, E, H, and S but rather, employing Eq. (5.2c,d), as functions of R and E only. The quasi-steady state approximation thereby returns our four-equation model to the form of our two-equation model. Moreover, we expect that even if such an approximation is not strictly permissible, so that the full four equation model of (4.2) and (5.1) must be solved to obtain accurate results, nonetheless qualitative behavior may well be similar to the situation where the approximation has in fact been made. Thus if we explicitly solve the four equation model, in cases where H and S change moderately rapidly, then it should often be the case that behavior similar to that obtained in our two-equation model will be evidenced.

Let us look at an example of the above considerations:

$$\begin{aligned}
\frac{dE}{dt} &= E(3.2 - 0.2E - R)(H - S) \ , \\
\frac{dR}{dt} &= R(0.4 - R + E)(7H - 13.5S + 0.5E^2 + 82) \ , \\
\frac{dH}{dt} &= \lambda H(6 - H + 2R + 3E) \ , \\
\frac{dS}{dt} &= \lambda S(8 - S + R + 2E) \ .
\end{aligned} \tag{5.3a,b,c,d}$$

In system (5.3) we exhibit four differential equations corresponding to four interacting cell populations, in particular including helper and suppressor cells. Note indeed that in Eqs. (5.3a) and (5.3b) an increase in the helper population H increases the proliferation rate of the cell populations E and R while an increase in the suppressor population S tends to decrease the proliferation rate, perhaps even shifting it

to negative values. Fig. 13 shows the network connections that are assumed by the model of system (5.3). Suppressive connections are shown as dashed arrows. In particular, each population has a self-limiting character of a logistic type. The effector population E is assumed to increase the population of the other three cell types. By contrast, the regulating population R suppresses E but enhances H and S.

If the parameter λ in (5.3c) and (5.3d) is sufficiently large, a good approximation should be obtained by making the quasi-steady state assumption $dH/dt = 0$, $dS/dt = 0$. Upon solving the resulting algebraic equations, we obtain (in addition to $H = 0,\ S = 0$)

$$H = 6 + 2R + 3E \ , \quad S = 8 + R + 2E \ . \qquad (5.4a,b)$$

Note that $H > 0,\ S > 0$ – as is necessary for biological realism. If the expressions of (5.4) are substituted into (5.3a,b), then, by design, model (4.4) is obtained. Given this, our previous discussion leads us to expect that solving the system (5.3) would lead to qualitative behavior that is similar to that shown in Figs. 9 and 10. Fig. 14, graphs of solutions to (5.3) with $\lambda = 100$, gives a partial demonstration that this in fact is correct. For example, Fig. 14A shows that adding a suitable number of effector cells in the diseased state can bring about a cure – in that the system returns to the vaccinated state. While carrying out these simulations, we were surprised to note the appearance of an alternative outcome that we have termed "over cure". As shown in Fig. 14B, if a number of effector cells greater than that of Fig. 14A is added to the diseased state, then the result is not a vaccinated state but rather a return to the normal state. This means that the organism would once again be susceptible to the disease. Of course this computer simulation does not take into account the possibility that effector cell levels could be so high on the way to "normalcy" that the animal would die well before normalcy was attained.

The reason for the unusual disease/normalcy transition can be traced to our original two variable model. This can be seen by referring to Fig. 5, the phase plane for the underlying model (4.4). It turns out that the separatrix emanating upward from S_1 bends around to the right in such a way that part of the domain of attraction of the normal state lies beyond the diseased state. The same phenomenon is seen in Fig. 6, which was developed after "over cure" was discovered.

5.1. Antigen Innoculation. Our minimal model can be expanded in another direction, to represent the induction of autoimmune disease by the injection of an appropriate antigen, for example, the induction of EAE by the injection of myelin basic protein (MBP). We do this by adding to the equation for the effector cells E a source term that is an increasing function of the antigen concentration A. This is certainly reasonable, for the effectors have been hypothesized to be driven by precisely this antigen. A third equation incorporates the assumption that the inoculated antigen disappears rapidly. Dispersion of the antigen and its removal by the immune system bring about this disappearance; since the details are not essential for our present purposes, we assume a simple exponential decay. The point is that the presence of the antigen will drive the effectors to a certain level E_0 at the time that the antigen has effectively disappeared. From then on the equations will be virtually identical to those of the minimal model, so the results should be essentially the same as those obtained by imposing an initial perturbation E_0 of E as an initial condition.

To check that our expectations are correct, we considered model (4.6), with the addition of antigen terms of the type discussed:

$$\begin{aligned}
\frac{dE}{dt} &= 0.01 + E(-0.05R - 0.05E^2 + 0.5125E + 0.125) + \frac{10A}{0.01 + A} \quad , \\
\frac{dR}{dt} &= 0.01 + R\left(0.35 - 0.05R + \frac{45E^2}{256 + E^4}\right) \quad , \qquad (5.5a, b, c) \\
\frac{dA}{dt} &= -20A \quad .
\end{aligned}$$

Initial conditions were

$$E(0) = E_N \quad , \quad R(0) = R_N \quad , \quad A(0) = A_0 \quad , \qquad (5.6a, b, c)$$

where E_N and R_N are "normal", effector and regulator steady states of (5.5a,b) with $A \equiv 0$.

Fig. 15A indeed shows that, according to model (5.5), a suitable dose of antigen to a normal animal can induce disease. We see in Fig. 15B that a smaller dose of antigen leads to vaccination. Note from (5.5c) that the time scale for antigen decay is $\tau = 0.05$. The first two arrows on the heavy trajectory in Fig. 15A are placed at intervals of $t = 0.1$. By $t = 0.2$, the antigen has decayed to a fraction of its

initial value A_0. Nonetheless, A_0 is so large that before it reaches negligible values, which takes many multiples of τ, the antigen drives the system past S_2 into the domain of attraction of the diseased state D. By contrast, in Fig. 15B, with the initial condition $A_0 = 1$, the antigen has virtually disappeared by $t = 0.2$; but by this time the state of the system has moved the short distance into the domain of attraction of the vaccinated state V. Apparently this route to vaccination has not been observed. The experiment would seem worth trying.

5.2. Inoculating Killed Cells. As another step toward expanding our minimal model in the direction of greater realism, let us consider the fact that T-cell vaccination is often carried out with killed and treated cells. In order to model this situation we assume that killed effectors can supplement the actions of live effectors, up to a point (i.e., in a saturating manner). To be precise, we replace E by $E + QD/(K + D)$ in (4.5a,b). Here D denotes the dead (killed) effectors. In addition, we assume that the dead cells are cleared from the system in a time of order $a^{-1}(dD/dt = aD)$. As expected, such equations can give rise to all the transitions listed in Table 1 (not shown).

6. Spontaneous Acquisition and Cure of Disease. Our analysis has been based on the identification of the normal, vaccinated, and diseased states of an animal with steady states of a suitable mathematical model. We discussed some of the limitations of this *steady state characterization* (not to be confused with the quasi-steady state assumption that was employed in Section 5). If the steady-state characterization is relaxed to some extent, our models can be extended to cover a larger group of phenomena, notably the spontaneous acquisition of disease in some animals and spontaneous cure in others. Examples of these phenomena are (i) the spontaneous acquisition of diabetes in about 90% of female NOD mice and 50% of the males (Elias et al., 1991), and (ii) the spontaneous return to health after some days in mice or rats in which EAE has been induced (Raine, 1984).

Let us now imagine that some or all of the constants in the basic model are in fact slowly varying functions of time. [This is a well known strategy in theoretical biology; for example in modeling the bursting oscillations of neurons (a classical and a recent reference are Rinzel, 1987, and Av-ron, Parnas, and Segel, 1993).] The slow variation of the "constants", reflecting slow changes in certain underlying biological processes, will lead to a slow distortion of the nullclines in the phase plane.

Suppose for definiteness that the main effect of this distortion is to elevate the right portion of the horizontal nullcline in Fig. 7, the diagram corresponding to model (4.5). This can be done, for example, by replacing (4.5b) by

$$\frac{dR}{dt} = R(-R + 0.02E^3 - \frac{1}{3}E^2 + CE + 1) \ , \tag{6.1}$$

where C is a slowly varying parameter. Suppose that C slowly increases from its value $C = 1.3$ of (4.5b). If the organism is in the diseased state D, then this state slowly moves leftwards and upwards (R increases and E decreases) until D and S_2 coincide and annihilate each other (see Fig. 16). The system now finds itself in the domain of attraction of V, so the vaccinated state will soon be attained. *Spontaneous cure* has taken place. The cure is predicted to occur in two stages: an initial slow increase in R and a concomitant decrease in E (Fig. 16A) followed by a period wherein much more rapid but similar changes in R and E lead to the vaccinated state (Fig. 16B). We note that assumption of faster and faster "slow distortions" brings about a transition from the present type of model, where disease is characterized by a "temporary steady state", to a model where the disease state is characterized by a transient high level of effectors.

Suppose that the underlying biological changes have the effect of depressing the left portion of the horizontal nullcline in Fig. 7 and that the organism is in the vaccinated state V. Then V slowly moves downwards and rightwards (R decreases and E increases) until V and S_2 coincide and annihilate each other, leaving the system in D's domain of attraction (see Fig. 17). The vaccinated animal will spontaneously pass from the vaccinated to the diseased state. Once again this is predicted to occur (if at all) in a two stage process – the first slow and the second fast.

Can slow distortions of nullclines bring about a "spontaneous" transition from *normal* to diseased? It seems not if, for example, model (4.5) of Fig. 7 is employed. The normal state N can be made to disappear by a descent of the left-most portion of the horizontal nullcline until N merges with the unstable steady state at the origin O. But then O becomes stable and takes over as the normal state. The origin persists as a steady state, regardless of the motion of the other nullclines, for all models of the form (4.2).

By contrast, the spontaneous appearance of disease in a normal animal is easily demonstrated by model (4.6) of Fig. 8. Sufficient elevation of the left portion of the vertical nullcline (relative to the horizontal nullcline) will result in the coalescence

and disappearance of states N and S_1 while elevation of the right portion of the vertical nullcline results in coalescence and disappearance of V and S_2 (Fig. 18A). This leaves the diseased state D as the only steady state. Depending on which coalescence occurs first, $V - S_2$ (as in Fig. 18 A and B) or $N - S_1$ (not shown), the normal-to-disease transition will occur directly or via the vaccinated state. See the Appendix for further discussion of the special features of model (4.6).

7. Summary and Discussion. As we have repeatedly stressed, the backbone of our modeling here has been the assumption that to first approximation the dynamical interactions between various classes of cells that are relevant to T-cell vaccination possess three stable steady states, corresponding respectively to a normal, vaccinated, and diseased organism. We have provided several specific examples [Eqs. (4.3)-(4.6)] from a class of minimal models all of which exhibit six transitions (Table 1) that are known to be characteristic of T-cell vaccination. A new transition has been discovered, "over cure", where treatment leaves the organism cured but susceptible.

We have demonstrated that a T-cell vaccination model that is comprised only of effector cells E does not work. There is a requirement for network effects, at least to the extent of adding a single "regulator"cell population R that responds to changes in the effector population level and that also influences the effectors. The cell population R might be anti-idiotypic cells bearing receptors that bind epitopes on the variable portion of the E receptors. Another possibility is that R represents anti-ergotypic cells (Lohse et al., 1993) stimulated by markers that indicate that the E cells are activated. Alternatively, the R cells can be influcenced by cytokines that are secreted by the E population or by a cell population that is influenced by the E's.

Section 5 shows that the two variable $E-R$ models can provide an approximate representation of the dynamics even if several other cell populations are involved. This can occur if the other populations respond relatively rapidly to their environment. Be that as it may, it is likely that an accurate model for a given auto-immune disease will eventually be found to contain numerous equations for various cell types and cytokines. Nonetheless, the idea of identifying the normal, vaccinated, and diseased phenomenologies with steady states of a dynamical system may remain valid and useful.

In all our models, the vaccinated state contains a level of effector cells that is elevated, but not so high as in disease. These cells are held in check by expanded populations of regulator cells. This is consistent with evidence that resistant organisms carry significant levels of effectors as well as other cells that specifically suppress them (Cohen, 1986).

We made some steps toward expanding the minimal model by considering the effects of additional helper and suppressor cell populations, of killed treated cells, and of antigen. Adoption of a quasi-steady state assumption for the dynamics of the additional helper and suppressor populations permitted us to design augmented systems whose qualitative behavior was essentially identical to the minimal system. In this context, the quasi-steady state assumption can be regarded as a scaffolding that allows us to determine major features of complex models that exhibit appropriate qualitative behavior. If time scales are changed in the model so that a quasi-steady state assumption becomes less and less appropriate, there is good ground to hope (as some examples have demonstrated – see Fig. 14) that appropriate qualitative behavior remains, perhaps after suitable parameter alteration.

In modeling the effects of inoculations of killed treated cells or of antigen, we introduced new equations to represent, respectively, these inoculants. Nonetheless, the basic interactions of effectors E and regulators R remained at the heart of the modeled behavior: by assumption, the inoculants mainly forced E and R to certain values before they disappeared. Extending this viewpoint, we see how the simple E, R model might capture much of the essence of certain autoimmune interactions even though other populations are certainly involved. For example inoculation of clone A2c can cure adjuvant arthritis; this clone does not directly suppress the effector clone but rather acts via an intermediate population (Cohen, 1986).

Relaxing the approximation that normality, vaccination, and disease are steady states permitted us to broaden the behavioral repertoire associated with our model. This "relaxation" amounts to assuming that constant coefficients in our minimal model are, in fact, slowly varying functions of time. In biological terms, the more comprehensive model takes into account relatively slow processes. "Slow processes" change on a time scale that is long compared, for example, to the time it takes in a normal animal for a sizable inoculant of effector cells to induce a level of effector cells that is characteristic of autoimmune disease. We have shown that if these slow processes are such that suitable changes in the nullclines are induced, then there

can arise a whole new set of "spontaneous" transitions among the three basic states of the model. These transitions are listed in Table 2.

We cited evidence that examples of these transitions occur, such as spontaneous cure in EAE and spontaneous acquisition of diabetes. The prediction that a spontaneously cured animal might not revert to the vaccinated state, but rather to the normal state, might help explain the frequent relapses that occur in EAE. (Another possibility is that such a prediction would emerge from a more comprehensive model with a more accurate representation of immune memory.) We do not know whether there is any evidence that a vaccinated animal might nevertheless spontaneously become diseased after sufficient time elapses.

We stress that spontaneous transitions may occur after seemingly inconsequential alterations in the proliferation rates. For example, comparison of Fig. 12 and Fig. 19 illustrates the quite small differences in the regulator proliferation rate P_R before and after spontaneous cure was induced in the model of (4.5a) and (6.1). Such matters are discussed more fully at the end of Section 4.3.

The severity of induced autoimmune disease is strongly affected by the number of cells in the inducing inoculant. This fact is not easily accommodated by our minimal models, with their fixed steady state representing disease, although the varying nature of transients preceding the steady state can give some freedom to model varying degrees of disease severity. The introduction of secondary slow variation, however, at least in principle allows the models to account for changes in the severity of disease. Secondary slow variations must also be involved to explain the observation (see Cohen, 1988, pp. 121-3) that with pressure treatment, but not without it, activated T cell vaccination was effective against normally disease-producing inoculations of anti-MBP T lymphocytes. (In both instances, vaccination protected against inoculants of MBP in complete Freund's adjuvant – inoculants that therefore presumably are less effective than anti-MBP T cells in driving the effector population.) In terms of our model, the pressure-treated cells must generate a relatively large domain of attraction to the vaccinated state. Modification of the domain of attraction can only occur via parameter variation – i.e., by interactions not directly considered here. Dose and pressure effects are thus two of numerous topics that must be dealt with in the next stage of our investigation.

T-cell vaccination only works for certain strains of mice and rats. In present terms, the reason why this might be the case can be exemplified by imagining that

at birth the nature of effector-regulator interaction in some strain corresponds to the situation depicted in Fig. 18A. Here there is no vaccinated steady state and, hence, no cellular inoculations can move the system into the (non-existent) domain of attraction of vaccination. The only hope would be somehow to precede inoculation by the induction of changes that would subtly shift the situation in Fig. 18A to one, such as that depicted in Fig. 7, that does possess a vaccinated state. That is, our modeling suggests that *there may in principle exist suitable pre-treatments that would render a previously recalcitrant strain susceptible to T-cell vaccination.* Moreover, the models may indicate the type of pre-treatment required. In the case of Fig. 18A, for example, in mathematical terms a vaccinated state will result if the central portion of the horizontal nullcline is elevated sufficiently so that it intersects the vertical nullcline twice more. Biologically, this would require that means be found suitably to expand to higher R the band of positive proliferation rates P_R, at intermediate values of the effector population E.

This paper is based on a relatively unusual "reverse engineering" approach to modeling wherein equations are generated with scant regard to what may be the underlying mechanism, solely to reproduce certain phenomenology with minimal complication. We have earlier sketched some of the central ideas of this approach and their implications (Segel, Jäger, and Cohen, 1993). A previous biological theory that implicitly adopts such an approach is the phenomenological model of Odell et al. (1981) for a cell element with two rest lengths.

Partially similar in spirit are studies that construct neural networks that have desirable biological properties. An example is the paper of Doya and Yoshizawa (1989) that extends back-propagation algorithms to yield a network that can approximate a desired dynamical output, such as a given superposition of several sinusoidal oscillations. The idea here is to take a step toward understanding the neural control of motor behavior.

Taken in its broadest sense, selecting a model to reproduce observations is a central preoccupation of theoretical science. When the observations are time series, Weigend and Gershenfeld (1993) provide an up-to-date account of recent progress. What is novel here and in the cited paper by Odell et al. (1981) is the emphasis on reproducing particular qualitative features of the systems under investigation, namely the existence of several steady states with certain constraints on their nature (e.g., the level of E should be relatively high in disease) and on the transitions

between them. In principle, if they were mandated by the biology, other types of qualitative behavior could be incorporated, such as excitability or limit cycle oscillations, which correspond to known features of the phase plane. To yield these features, suitable modifications of the model differential equations must be provided.

More traditional approaches to reproducing observations typically reduce to parameter estimation – whether by contemporary applications of neural network techniques, as in Doya and Yoshizawa (1989), or by more conventional error-decreasing algorithms. By contrast, here it is the model structure and not parameter selection that is of primary interest. We make no attempt at quantitative accuracy. Given our fragmentary knowledge of the systems in question and the schematic nature of our model, it would be ill-advised to seek detailed agreement with experiment.

It is natural to inquire as to the extent to which our models are unique. This has been partially discussed in the Appendix, where we showed that our various specific models can be obtained from one another by certain distortions of nullclines and separatrices. The form of the equations could be constrained further by specifying that the right-hand sides be polynomials or rational functions of minimal degree, or by requiring the minimal number of steady states that will suffice to obtain the desired behavior. [Model (4.6) fulfills this last criterion.] Given that our goal is to increase biological understanding, little return seems likely to repay the investment of further work in this direction.

We have sought a formally structured approach to estimating the behaviors that might be inherent in certain immunological systems. At this stage in the evolution of the thinking of experimental and theoretical biologists concerning these systems, rather than the quantitative aspects of mathematics, what seems more helpful are its conceptual and qualitative facets. We have tried to strike a balance between a considerable degree of simplicity in modeling, to limit the proliferation of possible behaviors, and a degree of underdetermination, to allow for surprise (such as "overcure.")

It is not essential to the reverse engineering approach to make the assumption that all identified states of the organism (such as "normal", "vaccinated", and "diseased") correspond to steady states of the model dynamical system. For example, in addition to the approach described here, we have modelled EAE by a pair of equations with two stable steady states ("normal" and "vaccinated") wherein a superthreshold perturbation of the normal state results in a sizable pulse of effectors

(disease), after which the system approaches the "vaccinated" steady state (not shown).

A serious disadvantage of the reverse engineering approach is obvious. It is dangerous to ignore modelling constraints that flow from even partial knowledge of mechanism, and indeed the ultimate goal of a modeling effort is to incorporate the most important of the relevant biological mechanisms. There are partially compensatory advantages. By freeing a theoretical explanation from particular phenomenology, one decreases reliance on what is often imperfectly understood biology. At the same time, one increases awareness that only certain types of global interactions are truly responsible for the observed behavior, not a particular instantiation of these interactions. A simple reverse engineering model may provide a valuable phenomenological module in a larger scale modeling effort – for example, an immunological module in a study of host-pathogen coevolution. Moreover, the reverse engineering results may well provide valuable guidance in the next stage of the research, wherein one strives to incorporate in the modeling salient information concerning the particular elements involved (cell populations, cytokines) and their interactions. Typically, the precise nature of the interactions is unknown. The results of the reverse engineering analysis can help one select from among a range of biologically reasonable assumptions those that have added plausibility owing to the fact that they lead to a variety of observed phenomenology.

We have begun the next step in the theoretical development, trying to see whether what could be in principle could also be in practice. That is, when one attempts to incorporate the essence of the biology "without looking at the answer", does there emerge the observed behavioral repertoire that characterizes T-cell vaccination? More precisely, the question is this: Can one obtain the observed transitions of Tables 1 and 2, and other qualitative and semi-quantitative features of T-cell vaccination, by adopting the salient and agreed features of the relevant biology such as the EAE regulatory circuitry of Kumar and Sercarz (1992)? Assumptions can and should be skewed with the aid of reverse engineering only to the extent that one does not stray beyond the inevitable imprecision in establishing what is "salient and agreed".

How can models of the type that we have put forward be challenged? Kinetic measurements would be invaluable, for they could be compared with model findings

such as those in Figs. 9 and 10. If it were possible, study of in vitro interactions between identified cell types would provide important model constraints.

Another type of suggested experiment involves subjecting an organism to various magnitudes of perturbation. Consider, for instance, the findings that certain doses of live effector cells that bring about disease in a normal animal do not cause disease in a vaccinated animal. Contemplation of the different domains of attraction naturally leads to the question, suppose that larger doses of live effector cells were given. Would the vaccinated state give way to a diseased state as is predicted by some versions of our models (see Fig. 15, for example)? Is it possible that, as would occur for example in the models of Fig. 8, addition of substantial amounts of effector cells can induce a transition from disease to normalcy ("over cure")? The model depicted in Fig. 15 suggests that attempts be made to induce vaccination by injecting suitable "lowish" doses of antigen.

Experimental results such as those by Howell et al. (1989) (that are concerned with vaccination by peptides from T-cell receptors) broadly justify the effector-regulator roles that we have assumed here. Moreover, as this work was in its final stages, we learned of a first precise demonstration that regulatory $CD4^+$ T-cells result from MBP immunization during recovery from EAE. These cells are specific to a dominant peptide in the T cell receptor of the effectors, and they specifically down-regulate proliferation responses to the dominant peptide in MBP (Kumar and Sercarz, 1993). This verification of some of the principal features of our model is gratifying. But a sterner experimental challenge stems from the requirement of our theory that for certain concentration ranges the regulatory cells should *enhance* the proliferation of the effectors (perhaps via other cell populations). Similarly, we require that at certain effector and regulator concentrations the effectors should *suppress* the proliferation of the regulatory cells. [This concentration-dependent enhancement and suppression might come from the interaction of helper and suppressor cells and/or from bell-shaped interaction functions of the type that are frequently employed in contemporary network models, for example by de Boer, Segel, and Perelson (1992).] It would be interesting to try to test these less evident properties of the network interactions that seem required to generate the phenomenology of T-cell vaccination.

ACKNOWLEDGEMENTS

Support is acknowledged from NIH grant AI28433 (to LAS) and US-Israel Binational Science Foundation, grant 89-146 (to LAS and EJ). The authors are grateful to A. Perelson for general immunological instruction and for valuable remarks on a draft manuscript. Sabbatical year support was provided by the Los Alamos National Laboratory (Center for Nonlinear Studies); the Santa Fe Institute extended further hospitality.

APPENDIX: "UNIQUENESS"

It is worth spending a little effort investigating to what extent our models are "unique". Let us take Eqs. (4.3) of Fig. 6 as a prototype. To insure a degree of brevity, we limit consideration to the interior of the positive quadrant in the (E, R) plane. Here the intersections of the five straight-line nullclines yield the five essential steady-state points N, V, D, S_1, and S_2.

The coefficients in the differential equations must satisfy certain inequalities to ensure that N, V, and D are stable nodes and that S_1 and S_2 are saddle points. Certain other requirements were mentioned in Section 4. An additional restriction on qualitative behavior is imposed by fixing zones I-IV where trajectories head respectively up and to the right, up and to the left, down and to the right, down and to the left:

$$\begin{aligned} I:\ P_E > 0,\ P_R > 0\ ; \quad & II:\ P_E > 0,\ P_R < 0\ ; \\ III:\ P_E < 0,\ P_R > 0\ ; \quad & IV:\ P_E < 0,\ P_R < 0\ . \end{aligned} \tag{A.1}$$

The location of zones I-IV for model (4.3) is depicted in Fig. 19. For model (4.3), and for all our models, the signs of P_E and P_R change when, respectively, vertical or horizontal nullclines are crossed. Thus the whole roman numeral pattern in Fig. 19 is determined when one imposes the requirements that solutions head inward for points sufficiently far from the origin on both vertical and horizontal axes.

Although there are a number of restrictions on the class of models that we are considering, a great deal of freedom remains. This is evident in the variety of specific models (4.3)-(4.6) that fulfill our various requirements. Nonetheless, as we shall now show, consideration of nullcline deformation shows that this set of models, particularly the first three, in a sense are all special cases of a single overall model.

Continuous deformation of the nullclines, the boundaries between the various zones, is usually expected to bring about only nonessential alterations in qualitative behavior. For this to be the case, it is of course necessary that the coefficient changes that drive the nullcline deformations are such that the existence and stability of the various steady states remain unaltered. As one example of nullcline deformation, suppose that points a and b in Fig. 19 are moved together until they coincide, after which the common point is raised above the E-axis to point c. Effectively, the two horizontal nullclines ea and fb have been replaced by a single curve whose lower portion is the dashed line near c. Similarly, one can effectively shrink the region III that previously extended to infinity by means of the dashed curve de. The three horizontal nullclines md, ea, and bf have thereby been replaced by a single N-shaped curve. This leads to the situation of Fig. 7, with the representative particular pair of differential equations (4.5).

As another example of nullcline deformation, let us begin again with Fig. 19 but this time shrink region IV back from infinity by means of a line gf. It is readily seen that we now have a situation essentially equivalent to that of Fig. 6 with representative Eqs. (4.4). Thus, Eqs. (4.3), (4.4), and (4.5) are three representatives of a single class of models that can be regarded as topologically equivalent.

We emphasize that topologically equivalent models are not necessarily equivalent in the biological behavior that they predict. An example is furnished by the remark in the paragraph preceding (4.3) that the transition DIV occurs if and only if certain geometric requirements on one of the separatrices is fulfilled.

The transition from the "straight line" model (4.3) to (4.6) is more extensive than the transitions to models (4.4) and (4.5). The effect of the transition can readily be seen if we begin with the transformed version of Fig. 19 that in essence yielded Fig. 7. Let us slide together points h and k on the R axis. If the common point is then moved rightwards, we obtain a diagram of the type shown in Fig. 20A. The next step is obtained by moving point S_3 rightwards, off to infinity, and point U leftwards and upwards to a position on the R axis (Fig. 20B). Note that the points U and S_3 cease to be steady states after the transformations just specified.

The final stage in obtaining (4.6) is the introduction of small constant terms. Such a term in the dE/dt equation (4.6a) eliminates the vertical nullcline that formed the lower portions of the vertical axis (thereby removing the steady point at

the origin) and effectively merges the upper portion of this nullcline with the bell-shaped vertical nullcline of Fig. 20B. By contrast, the addition of a small constant term in the dR/dt equation has almost no effect. A small distortion of the cubic-shaped horizontal nullcline is induced. In addition, the E ceases to be a horizontal nullcline, but no qualitative effect results since this particular nullcline is no longer intersected by any vertical nullclines.

LITERATURE

Alborán, M. D., J. C. Gutierrez, J. A. Gonzalo, J. L. Andreu, M. A. R. Marcos, G. Kroemer, and C. Martinez-A. 1992. lpr T-cells vaccinate against lupus in MRL/lpr mice. *Eur. J. Immunol.* **22**, 1089-1093.

Av-Ron, E., H. Parnas, and L. A. Segel. 1993. A basic biophysical model for bursting neurons. *Biological Cybernetics.* In press.

Ben-Nun, A., H. Wekerle, and I. R. Cohen. 1981. Vaccination against autoimmune encephalomyelitis with T lymphocyte line cells reactive against myelin basic protein. *Nature* **292**, 60-61.

Beraud, E., O. Lider, E. Baharav, T. Reshef, and I. R. Cohen. 1989. Vaccination against experimental autoimmune encephalomyelitis using a subencephalitogenic dose of autoimmune effector cells. I. Characteristics of vaccination. *J. Autoimmunity* **2**, 75-86.

Cohen, I. R. 1986. Regulation of autoimmmune disease: Physiological and therapeutic. *Immunol. Rev.* **94**, 5-21.

Cohen, I. R. 1988. *Perspectives on Autoimmunity.* Boca Raton, Florida: CRC Press.

Cohen, I. R. and H. Atlan. 1989. Network regulation of autoimmunity: an automaton model. *J. Autoimmunity* **2**, 613-625.

de Boer, R. J., L. A. Segel, and A. S. Perelson. 1992. Pattern formation in one- and two-dimensional shape space models of the immune system. *J. Theoret. Biol.* **155**, 295-333.

Doya, K. and S. Yoshizawa. 1989. Adaptive neural oscillator using continuous-time back-propagation learning. *Neural Networks* **2**, 375-385.

Elias, D., T. Reshef, O. S. Birk, R. van der Zee, M. D. Walker, and I. R. Cohen. 1991. Vaccination against autoimmune mouse diabetes with a T-cell epitope of the human 65-kDa heat shock protein. *Proc. Natl. Acad. Sci. USA* **88**, 4577-4580.

Howell, M. D. , S. T. Winters, T. Olee, H. C. Powell, D. J. Carlo, S. W. Brostoff. 1989. Vaccination against experimental allergic encephalomyelitis with T-cell receptor peptides. *Science* **246**, 668-670.

Kumar, V. and E. E. Sercarz. 1992. T cell regulatory circuitry: Antigen-specific and TCR-idiopeptide-specific T cell interactions in EAE. *Interntl. Rev. Immunol.* **9**, 269-279.

Kumar, V. and E. E. Sercarz. 1993. TCR-peptide-specific regulatory $CD4^+$ T cells are involved in recovery from antigen-induced autoimmune disease. Submitted.

Lider, O., M. Shinitzky, and I. R. Cohen. 1986. Vaccination against experimental autoimmune diseases using T lymphocytes treated with hydrostatic pressure. *Ann. N. Y. Acad. Sci.* **475**, 267-273.

Lohse, A. W., T. W. Spahn, T. Wölfel, J. Herkel, I. R. Cohen, and K. H. Meyer zum Büschenfelde. 1993 Induction of the anti-ergotypic response. *International Immunology* **5**, 533-539.

Naparstek, Y., A. Ben-Nun, J. Holoshitz, T. Reshef, A. Frenkel, M. Rosenberg, and I. R. Cohen. 1983. T lymphocyte lines producing or vaccinating against autoimmune encephalomyelitis (EAE): Functional activation induces PNA receptors and accumulation in the brain and thymus of line cells. *Eur. J. Immunol.* **13**, 418-423.

Offner, H., G. A. Hashim, A. A. Vandenbark. 1991. T-cell receptor peptide therapy triggers autoregulation of experimental encephalomyelitis. *Science* **251**, 430-432.

Odell, G., G. Oster, P. Alberch, and B. Burnside. 1981. The mechanical basis of morphogenesis. I. Epithelial folding and invagination. *Dev. Biol.* **85**, 446-462.

Raine, C. S. 1984. Biology of disease. Analysis of autoimmune demyelination: its impact upon multiple sclerosis. *Laboratory Investigation* **50**, 608-635.

Rauch, J. G. 1993. The law on reverse engineering. *IEEE Spectrum* **30**, 47-8.

Rinzel, J. 1987. A formal classification of bursting mechanisms in excitable systems. *Mathematical Topics in Population Biology. Morphogenesis and Neurosciences*, E. Teramoto and M. Yamaguti (eds), Lecture Notes in Biomath. **71**, pp. 267-281. Berlin: Springer-Verlag.

Segel, L. A. and M. Slemrod. 1989. The quasi-steady state assumption: a case study in perturbation. *SIAM Rev.* **31**, 446-447.

Segel, L. A., E. Jäger, and I. R. Cohen. 1993. A kinetic model of T cell vaccination and autoimmune disease. Unpublished.

Wiegand, A. S. and N. A. Gershenfeld, eds. 1993. *Time Series Prediction: Forcasting the Future and Understanding the Past.* Reading, MA: Addison Wesley.

Table 1. Properties of T Cell Vaccination

Original state	Inoculant size	Type[1]	Resulting State	Mnemonic
Normal	small	L,K	Normal	NsN
Normal	medium	L	Vaccinated	NmV
Normal	large	L	Diseased	NlD
Vaccinated	large	L,K	Vaccinated	VlV
Diseased	small	L,K	Diseased	DsD
Diseased	large	K	Vaccinated	DlV

[1] L=live; K=killed and treated

Table 2. Spontaneous Transitions in Autoimmune Disease

Original State	Final State	Transition
Diseased	Vaccinated	Spontaneous cure
Normal	Diseased	Spontaneous disease
Vaccinated	Diseased	Spontaneous disease
Normal	Vaccination	Spontaneous vaccination

FIGURE CAPTIONS

Figure 1. "Phase line" for a one-variable model of T-cell vaccination showing the normal (N), vaccinated (V), and diseased (D) stable steady states of the effector population E, separated by unstable steady states S_1 and S_2. (Here and below, stable and unstable steady states are denoted by filled and unfilled circles, respectively.) The mnemonics of Table 1 are employed to indicate the various predicted transitions. For example, NmV indicates that a *m*edium perturbation to the *N*ormal state of the effector population (starting from the intersection of the dashed line labelled "NmV" with OE) is such that as time goes on the effector population moves in the direction of the arrows and thus tends to the *V*accinated state.

Figure 2. Schematic version of phase plane requirements for a two-variable model (with a cell population R regulating the effectors E) of the general form (4.1).

Figure 3. Schematic diagram of horizontal and vertical nullclines, the loci of points where trajectories are respectively vertical and horizontal. As shown, steady state points occur at the intersections of such nullclines.

Figure 4. A: Typical separatrix, with saddlepoint S (see inset for more detail). The separatrix divides the two classes of trajectories NsN and NmV. B: Representation of the salient requirements on the phase plane representation of the assumed form of model (4.2).

Figure 5. Phase plane corresponding to model (4.3). Here and in Figs. 6-8 the domains of attraction of the steady state points N, V, and D are respectively hatched, unmarked, and stippled. Note that the essential requirements of Fig. 4B indeed appear in Fig. 5 (although the orientations of the nullclines are quite different) – as is the case in Figs 6-8.

Figure 6. Phase plane diagram corresponding to model (4.4).

Figure 7. Phase plane diagram corresponding to model (4.5).

Figure 8. Phase plane diagram corresponding to model (4.6). As with previous models, a sufficiently large perturbation of the diseased state (starting at A) will yield an approach to the vaccinated state and, hence, cure. But here an even larger

perturbation, starting at B, results in a return to the normal state, leaving the possibility of renewed disease ("over cure").

Figure 9. Standard plots of the development with time of various initial perturbations, illustrating the cases of Table 1. Model (4.1) has been used for the computer calculations, but similar results are found for models (4.3), (4.5), and (4.6). On the right side of the graphs are indicated the E and R values for relevant N, V, and D steady states. A: NsN. B: NmV. C:NlD.

Figure 10. Similar to Fig. 9. A: VlV. B: DsD. C:DlV. Note that the same initial effector population results in disease in Fig. 9C, but vaccination in Fig. 10A.

Figure 11. Dependence of the effector proliferation rate P_E on the effector (E) and regulatory cell (R) population levels for system (4.5). A: Three-dimensional plot of P_E. B: Three-dimensional plot of P_E when $P_E > 0$. C: Region of (E, R) plane where P_E is positive (hatched) and negative (clear).

Figure 12. Counterpart of Fig. 11 for P_R, the proliferation rate of the regulatory cells.

Figure 13. The network of four cell populations, including helpers H and suppressors S, that is assumed in model (5.3).

Figure 14. Graphs for solutions to the four variable model (5.3) with $\lambda = 100$. The asymptotic values of the four populations, the steady state levels in vaccination and disease, are indicated on the right vertical line. A: Cure (DlV). B: "Over cure" – An even larger addition of effector cells brings about a return to the normal state.

Figure 15. Effect of antigen inoculation in a normal animal according to model (5.5) with initial conditions (5.6). The initial antigen level was $A_0 = 5000$ in A and $A_0 = 1$ in B, resulting respectively in disease and vaccination for large and small inoculations. Heavy lines delineate the resultant trajectories in the phase plane appropriate for (5.5a,b) with $A \equiv 0$.

Figure 16. Illustration of spontaneous cure by slow variation of coefficient C in (4.5a) and (6.1) and concomitant slow distortion of nullclines. A: Slow elevation of the right portion of the horizontal nullcline has changed Fig. 7 ($C = 1.3$) to the depicted configuration ($C = 1.38$). During this distortion, the state of the system Δ remains at the diseased point D, which moves slowly upward and leftward. B: The

phase plane just after further slow nullcline elevation ($C = 1.4$) has led to the merger of the steady states D and S_2 and, hence, their mutual annihilation. The domain of attraction of D (stippled) has been swallowed by that of V (unmarked). The state of the system is now represented by an "ordinary initial condition" Δ within the domain of attraction of V. Thus the system will rapidly tend to the vaccinated state along some trajectory indicated schematically by a heavy line.

Figure 17. Schematic illustration of spontaneous acquisition of disease from the vaccinated state. A: Effect of slow descent of the left portion of the horizontal nullcline in Fig. 7. The state of the system, Δ, is assumed to be at the vaccinated point V. B: Further changes lead to the disappearance of the vaccinated state V, by merger with S_2, and rapid progression of the system state to disease (heavy line), since Δ is in D's domain of attraction.

Figure 18. Schematic illustration of spontaneous acquisition of disease from the normal state. A: A version of Fig. 8 in which elevation of the left-central portion of the vertical nullcline has resulted in the coalescence and disappearance of V and S_2. The system is in the normal state Δ. B: Elevation of the left portion of vertical nullcline leads to the coalescence and disappearance of N and S_1. Rapid progression to disease ensues (schematically indicated by the heavy line trajectory).

Figure 19. The nullclines for system (4.3) and the corresponding zones where trajectories head up and to the right (I), up and to the left (II), down and to the right (III), down and to the left (IV). Other material relates to the distortions of the nullclines to yield other models; see text.

Figure 20. Schematic illustration of two intermediate stages in the transformation of Fig. 7 [the phase plane for system (4.3)] to Fig. 8 [the phase plane for system (4.6)]. See text.

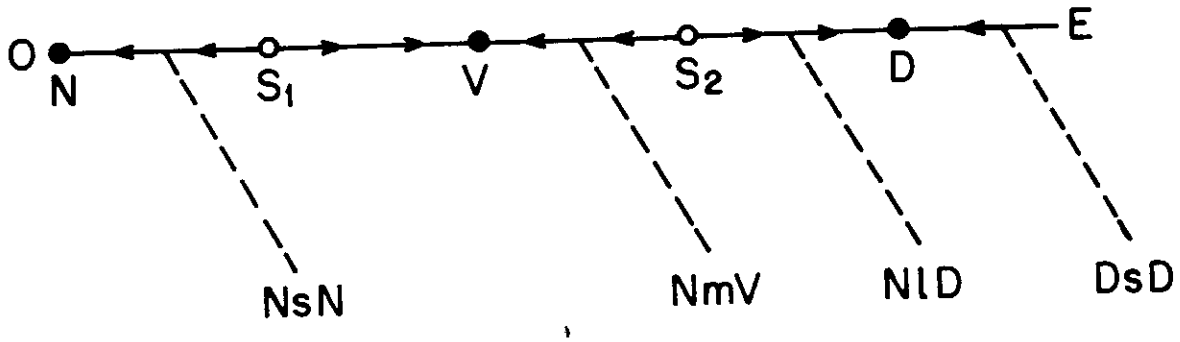
O
N
S1
V
S2
D
E
NsN
NmV
NlD
DsD

Fig. 1

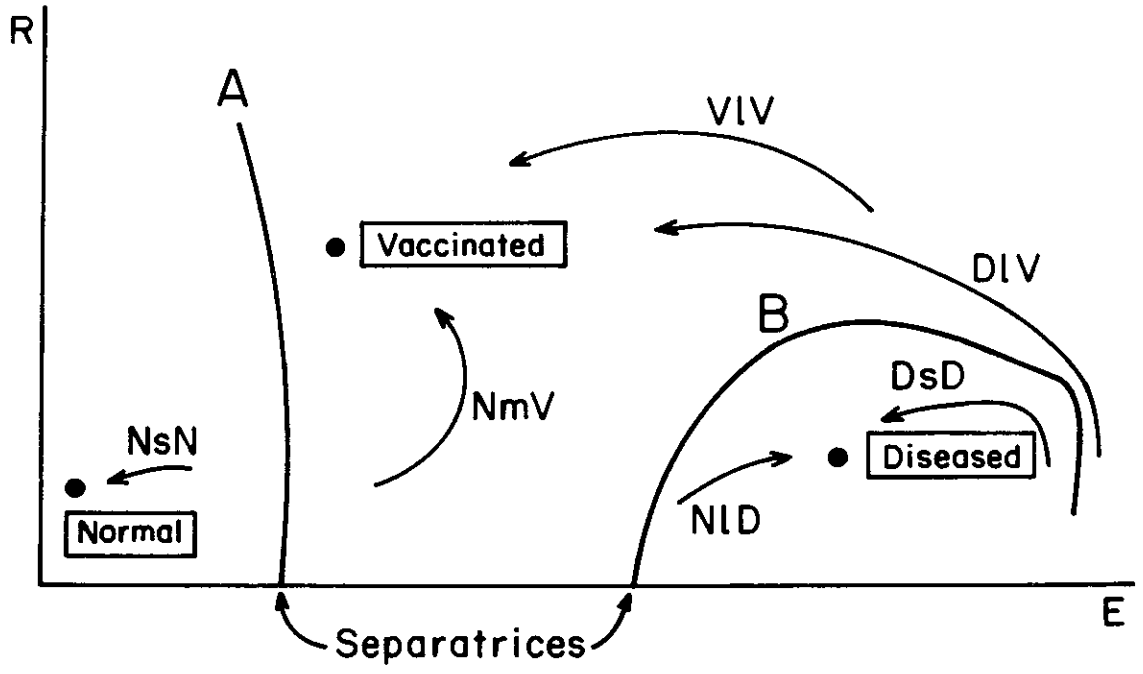
R
A
VlV
Vaccinated
DlV
B
DsD
NmV
NsN
Diseased
Normal
NlD
E
Separatrices

Fig. 2

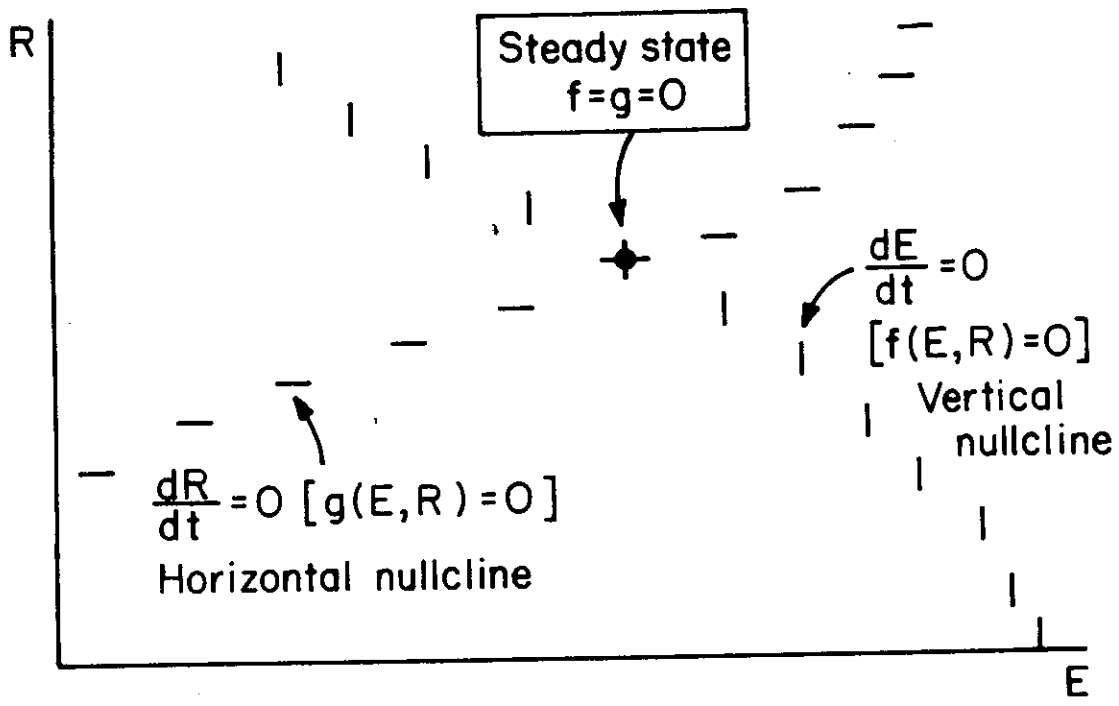
R
Steady state
f=g=0
dE/dt =0
[f(E,R)=0]
Vertical
nullcline
dR/dt =0 [g(E,R)=0]
Horizontal nullcline
E

Fig. 3

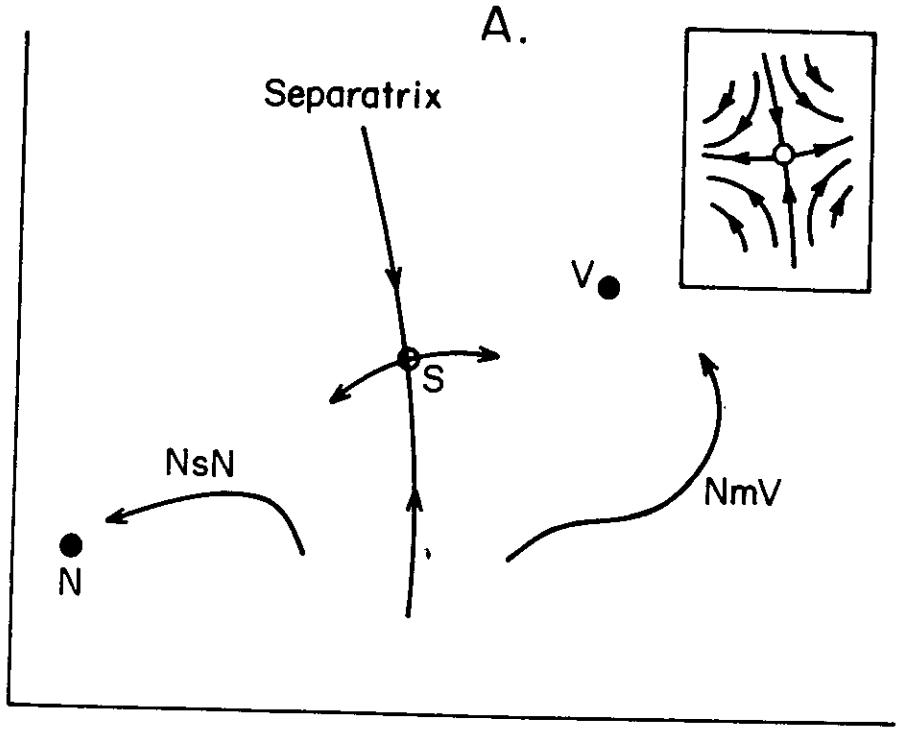
A.
Separatrix
V
S
NsN
NmV
N

Fig. 4

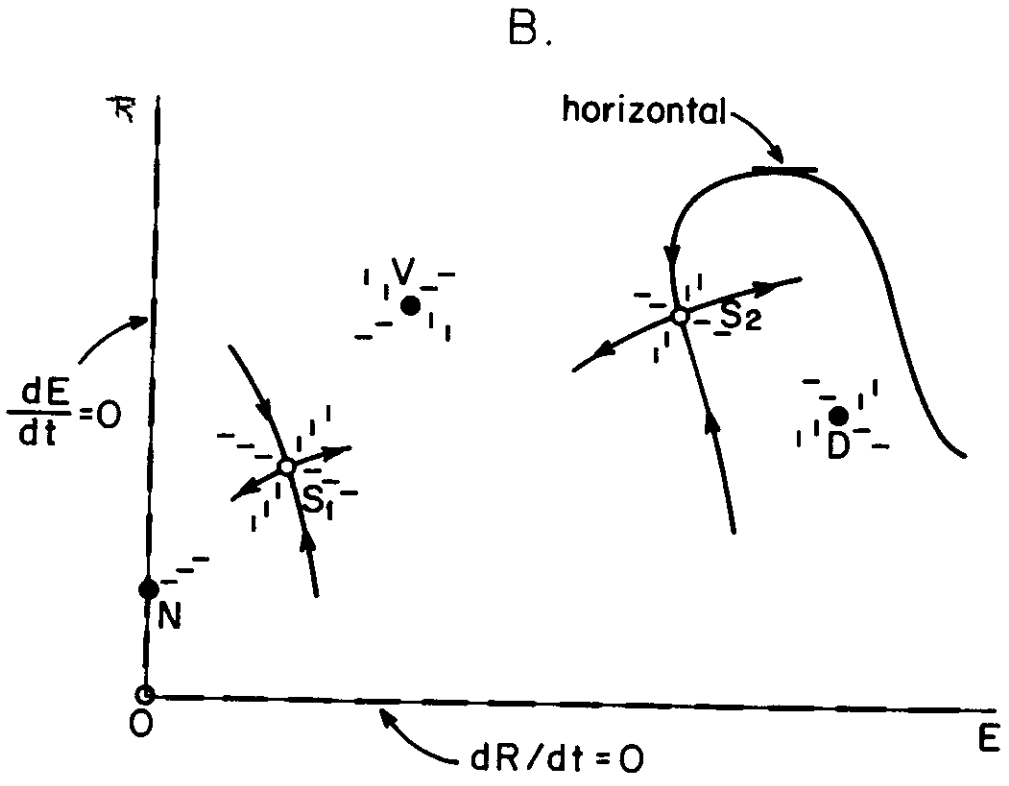
B.
R
horizontal
V
S2
dE/dt=0
D
S1
N
O
E
dR/dt=0

Fig. 4

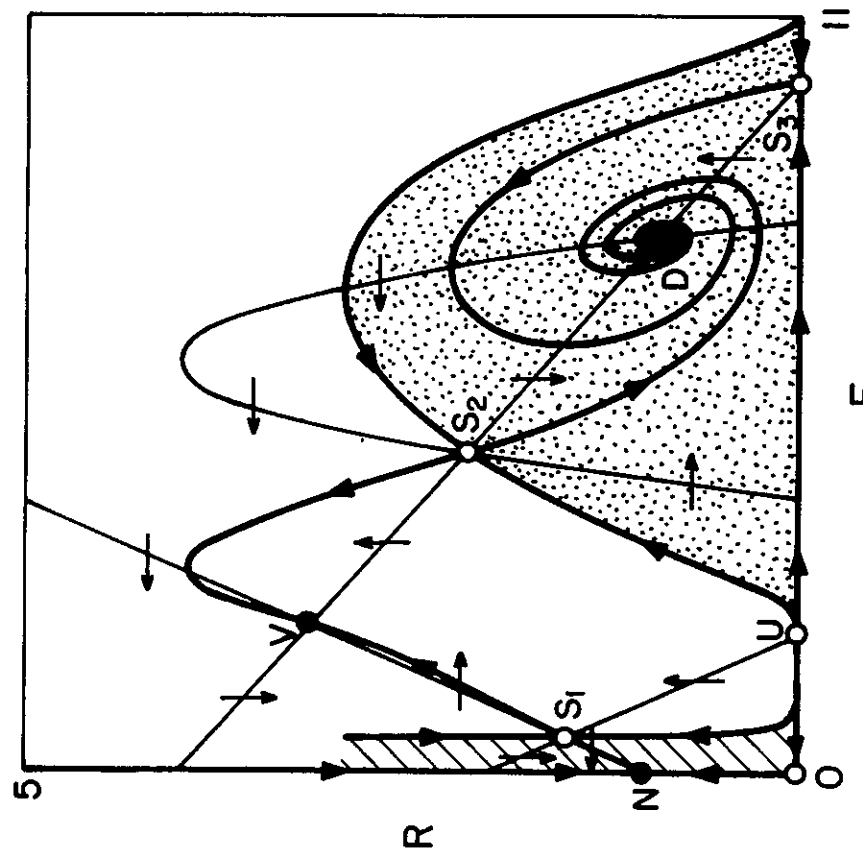

Fig. 6

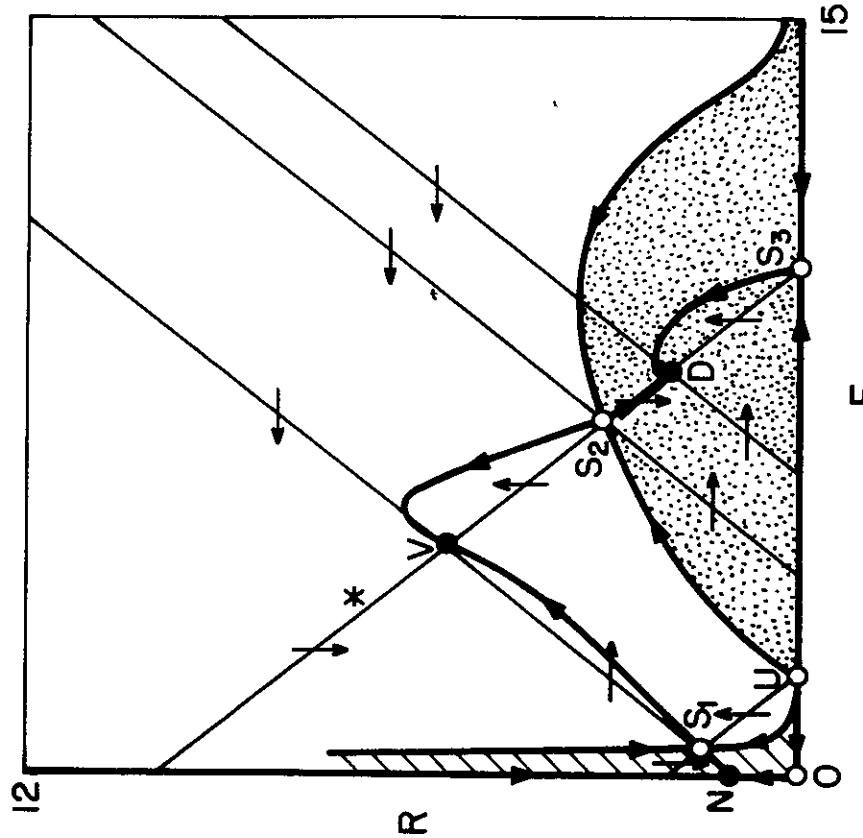

Fig. 5

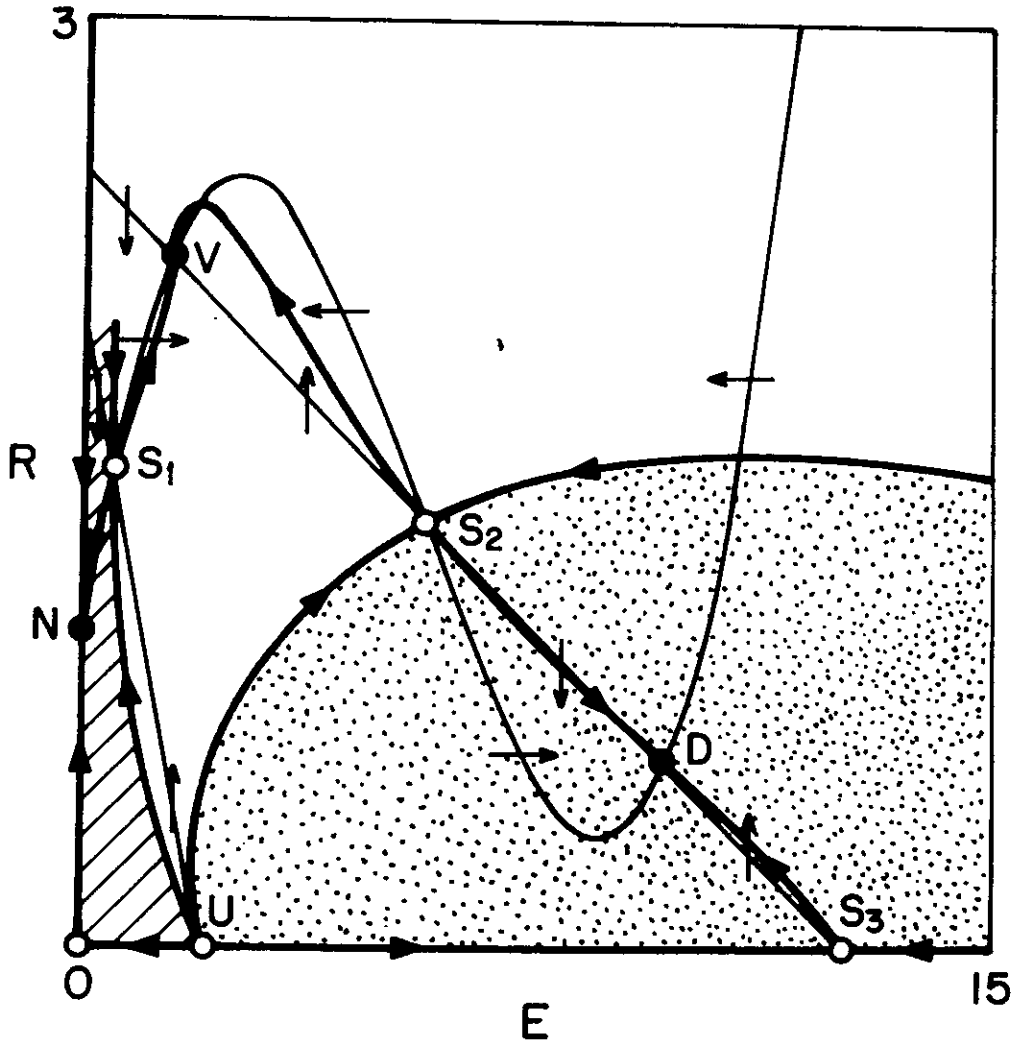

Fig. 7

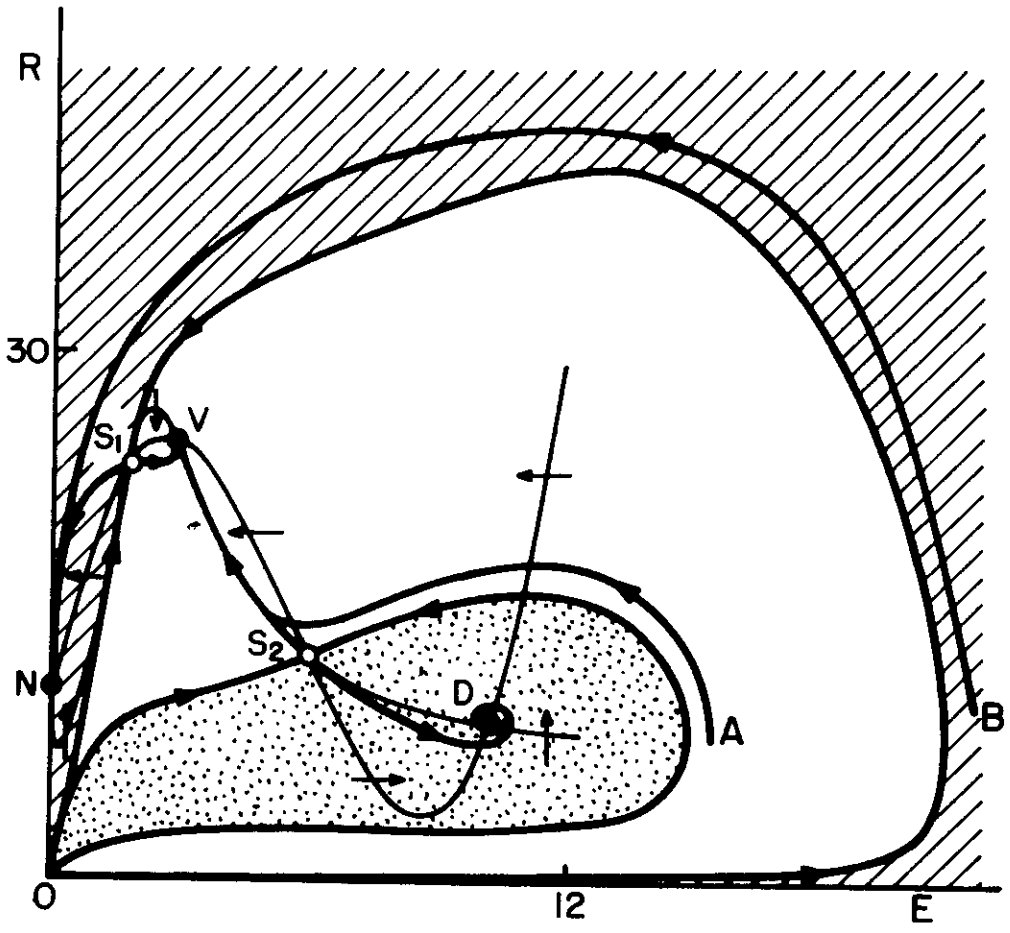

Fig. 8

A.

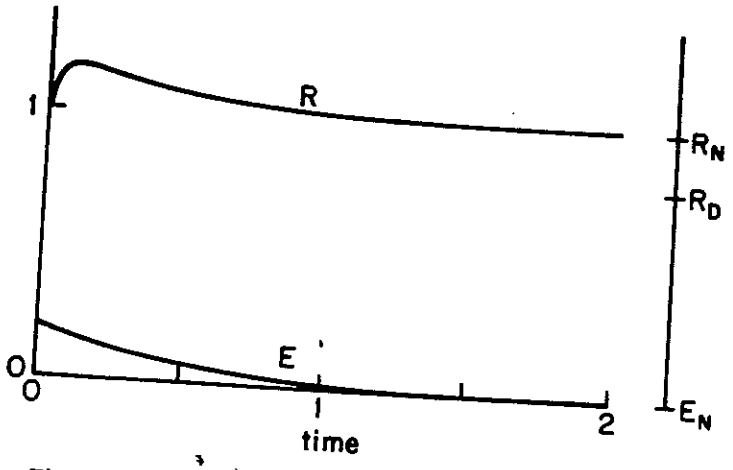

Fig. 9

B.

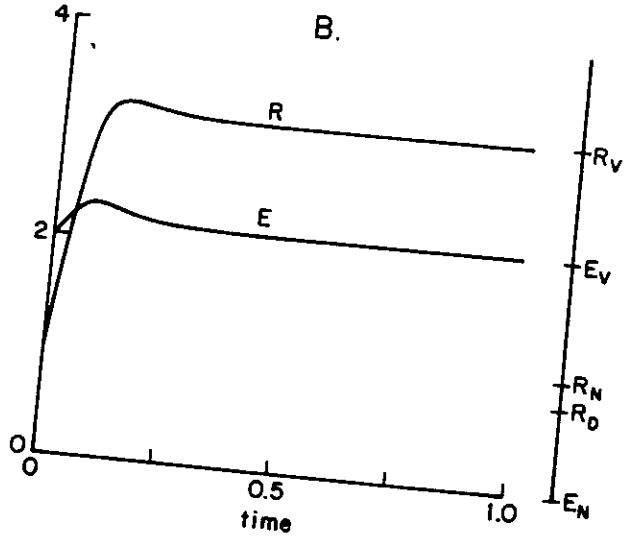

Fig. 9

C.

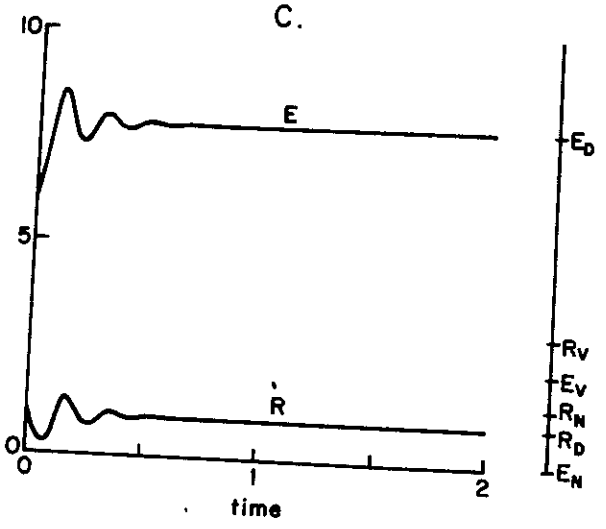

Fig. 9

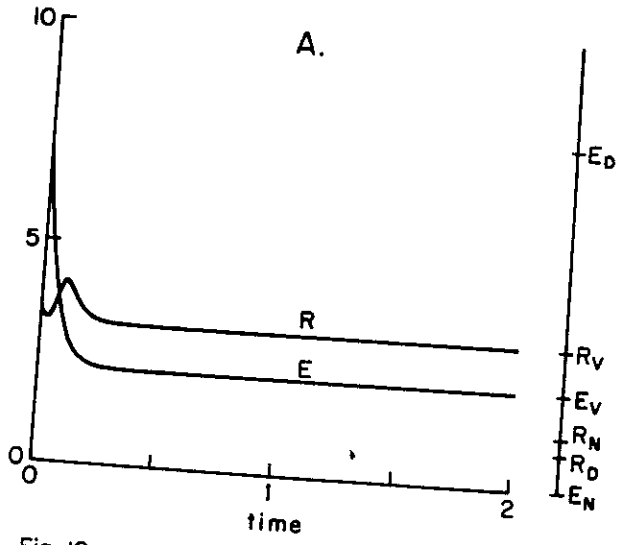

Fig. 10

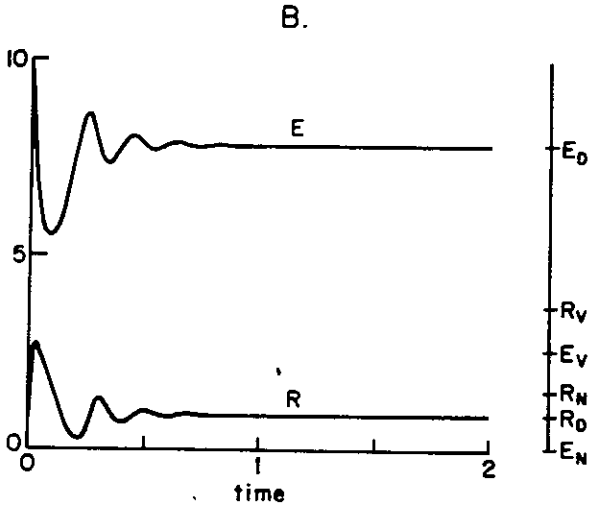

Fig. 10

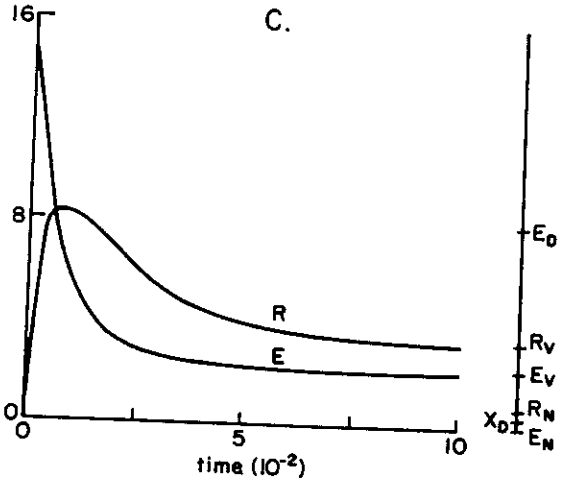

Fig. 10

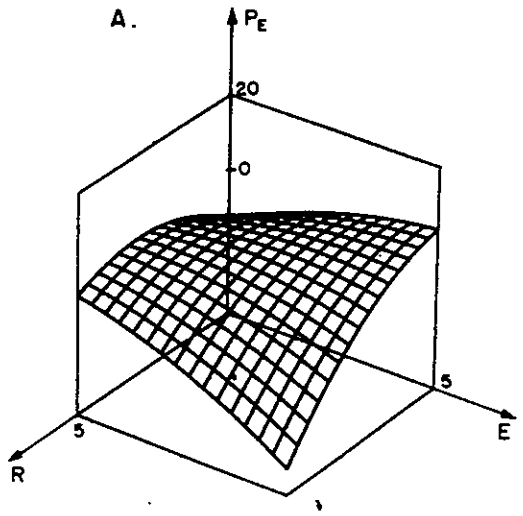

Fig. 11

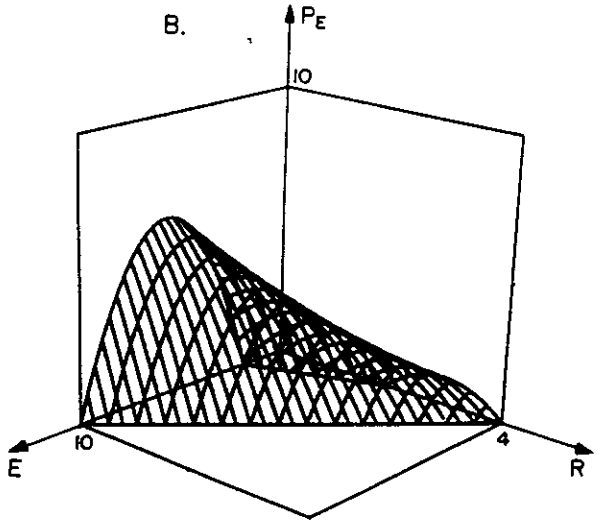

Fig. 11

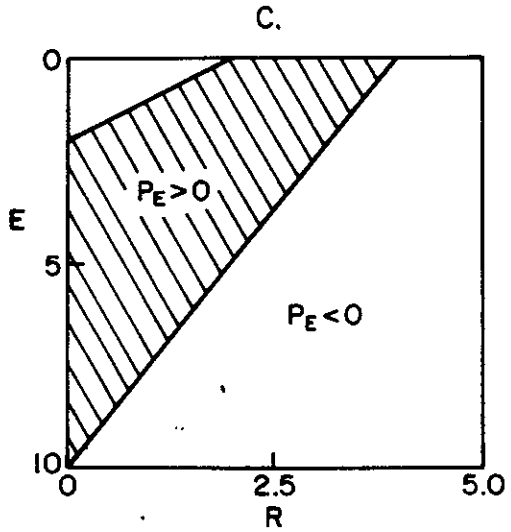

Fig. 11

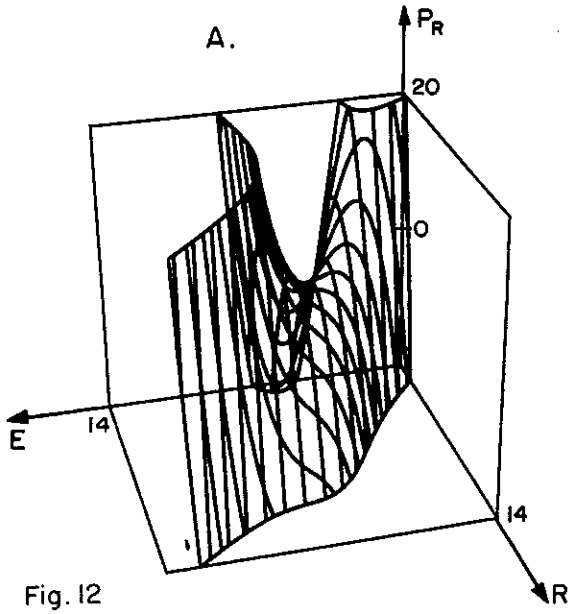

Fig. 12

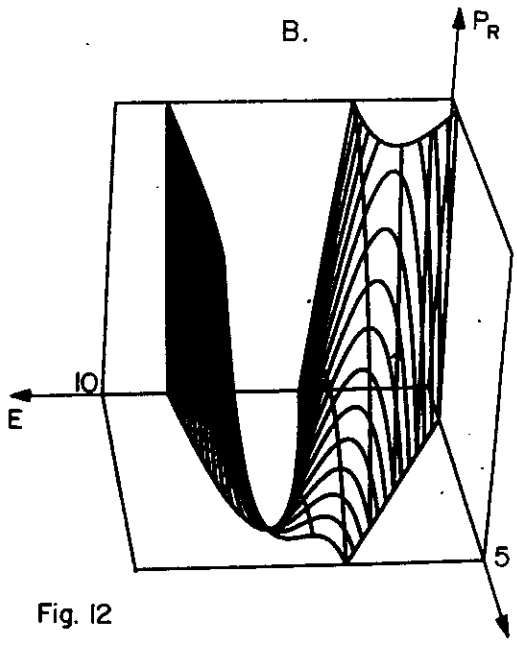

Fig. 12

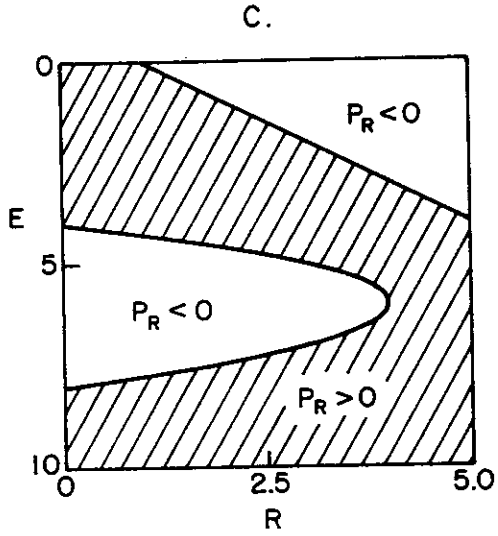

Fig. 12

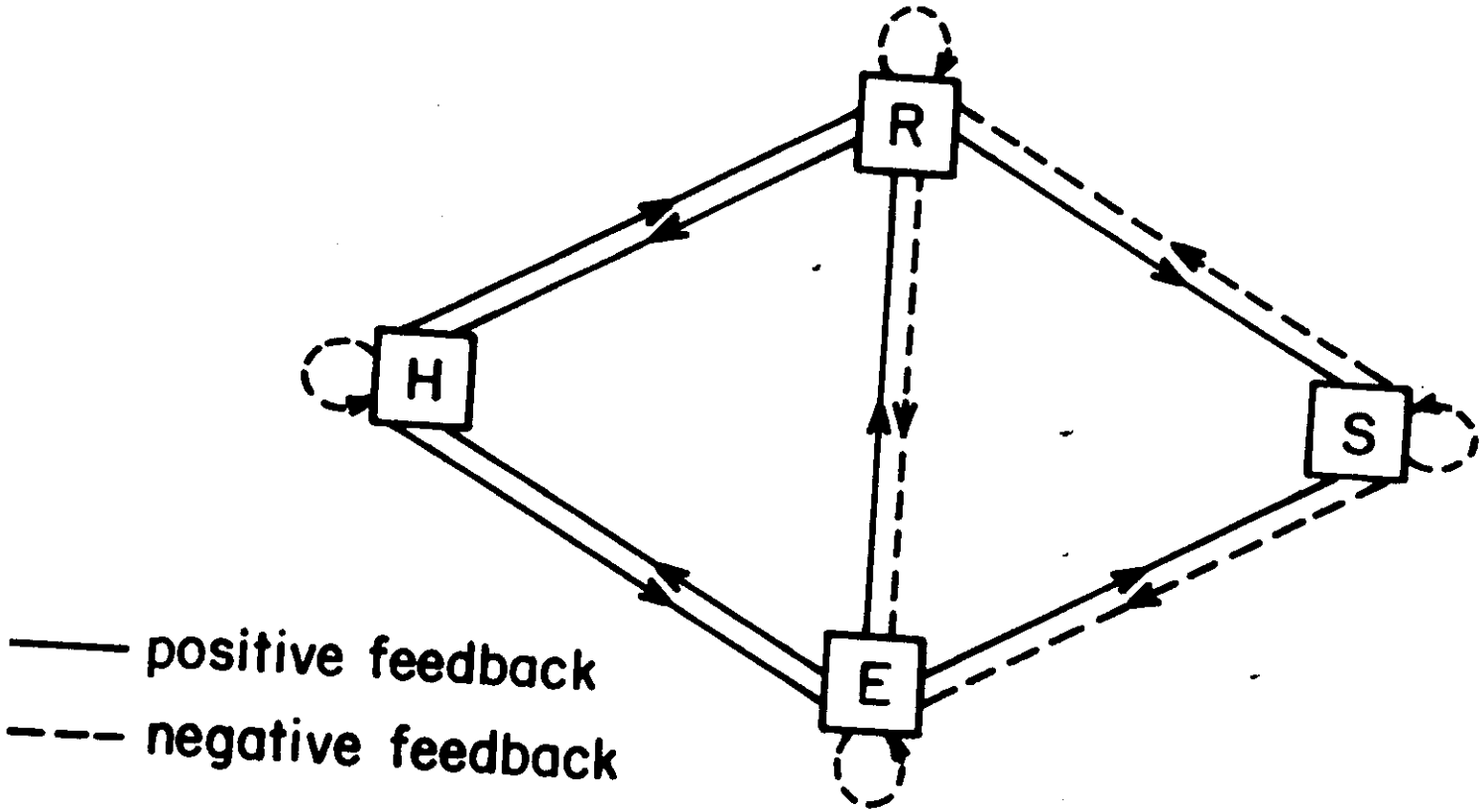

Fig. 13

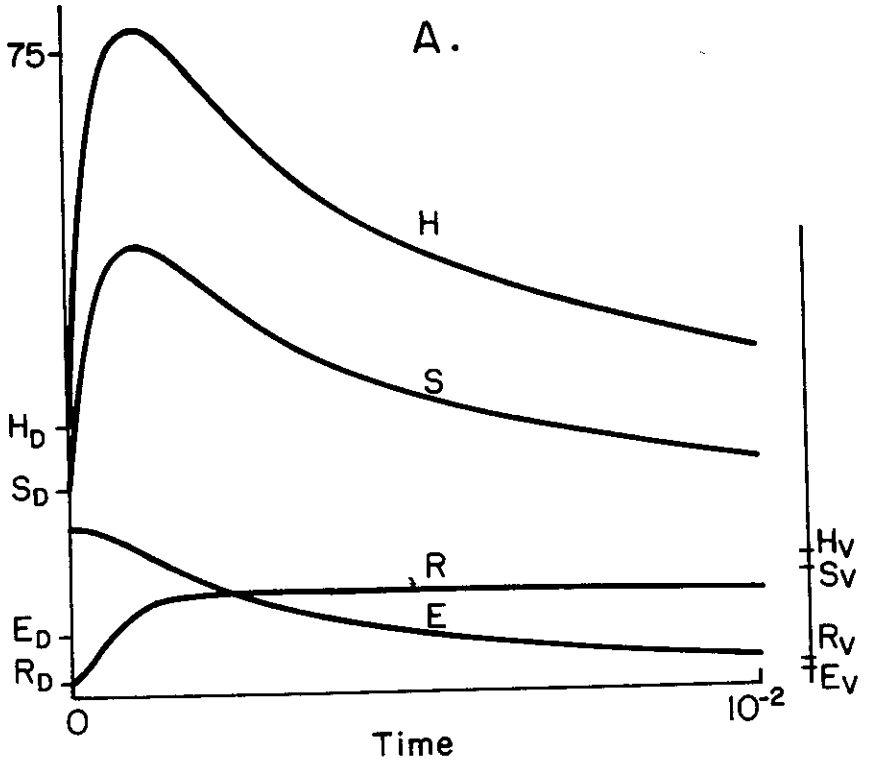
A.
75
H
S
H_D
S_D
R
E
E_D
R_D
H_V
S_V
R_V
E_V
0
10^{-2}
Time

Fig. 14

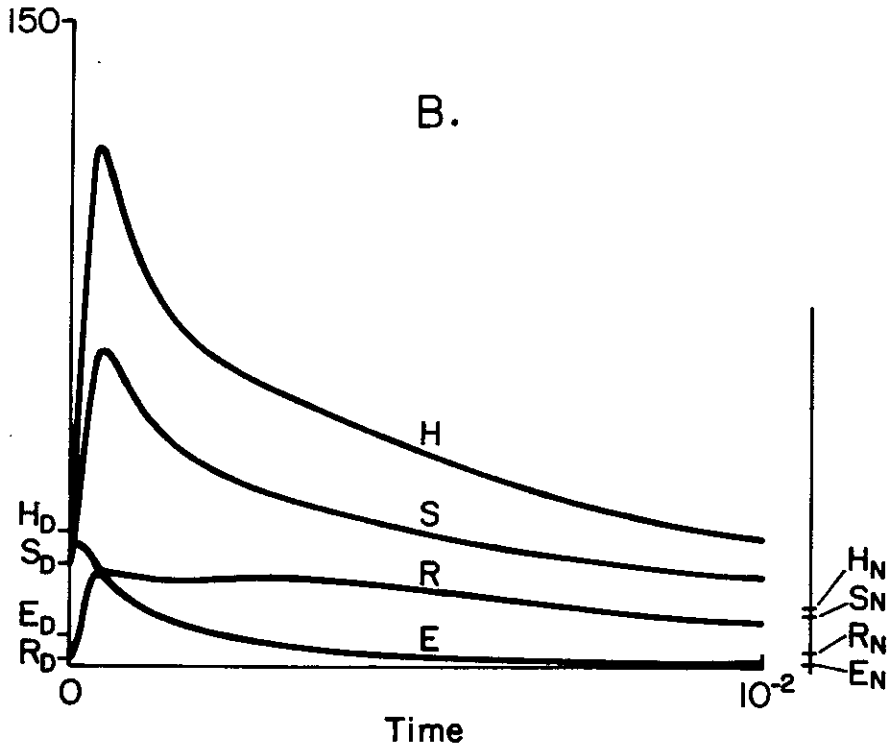
150
B.
H
S
R
E
H_D
S_D
E_D
R_D
H_N
S_N
R_N
E_N
0
10^{-2}
Time

Fig. 14

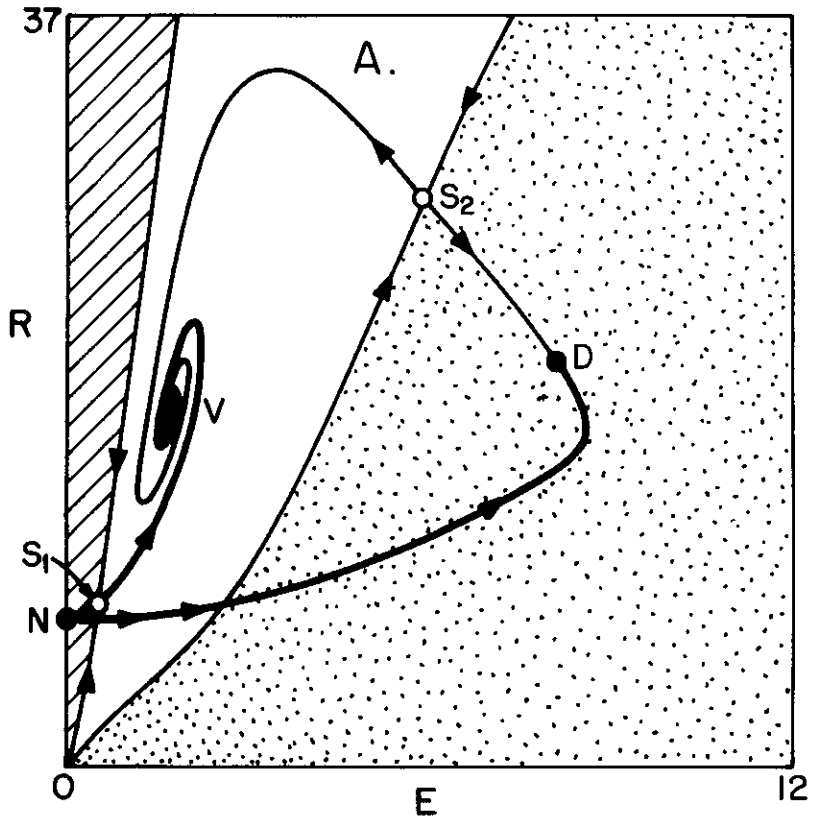

Fig. 15

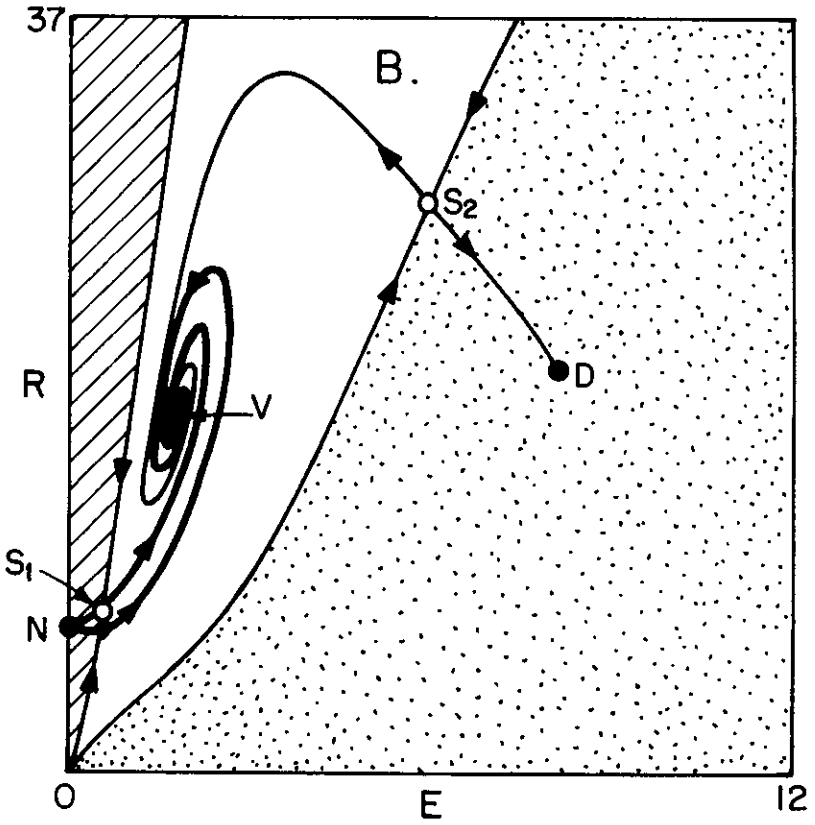

Fig. 15

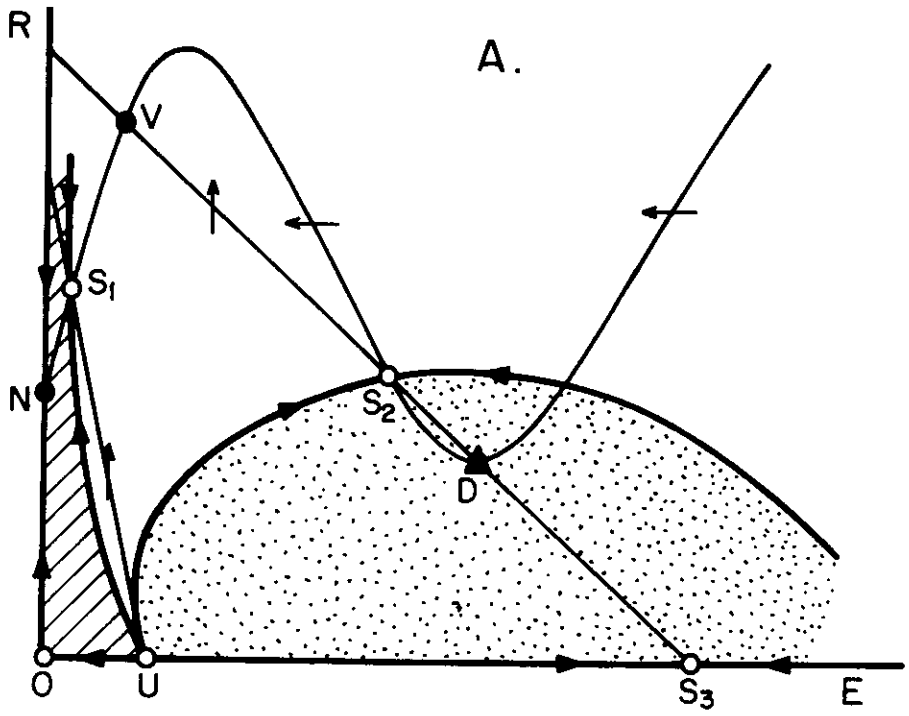

Fig. 16

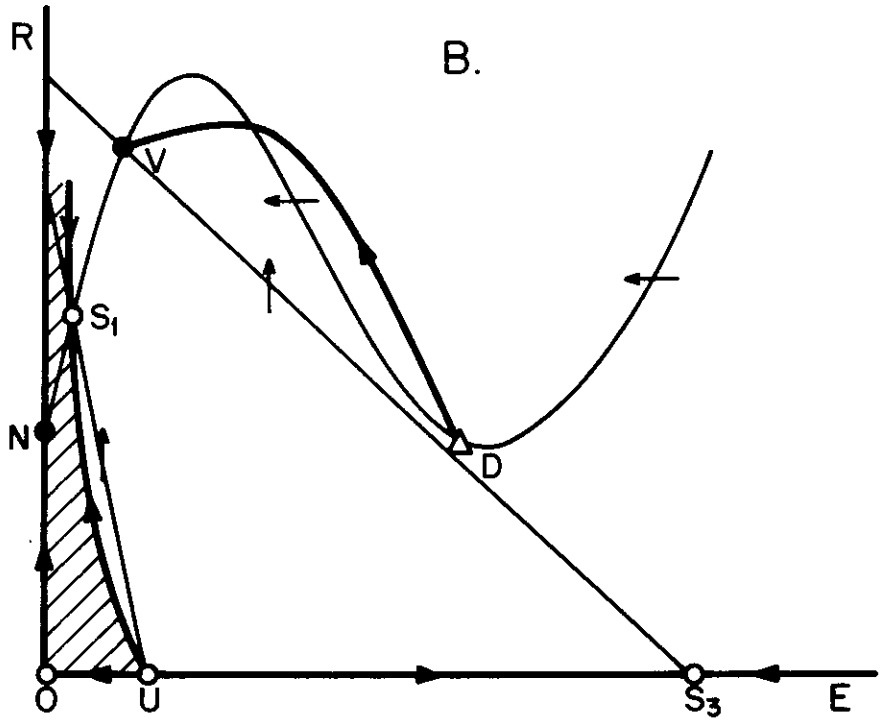

Fig. 16

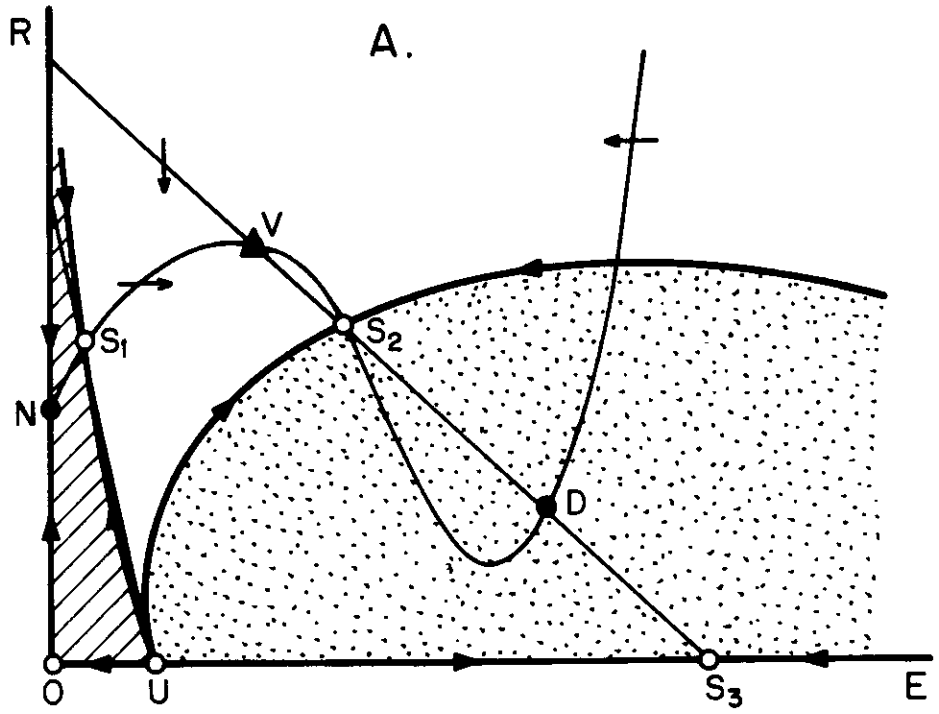

Fig. 17

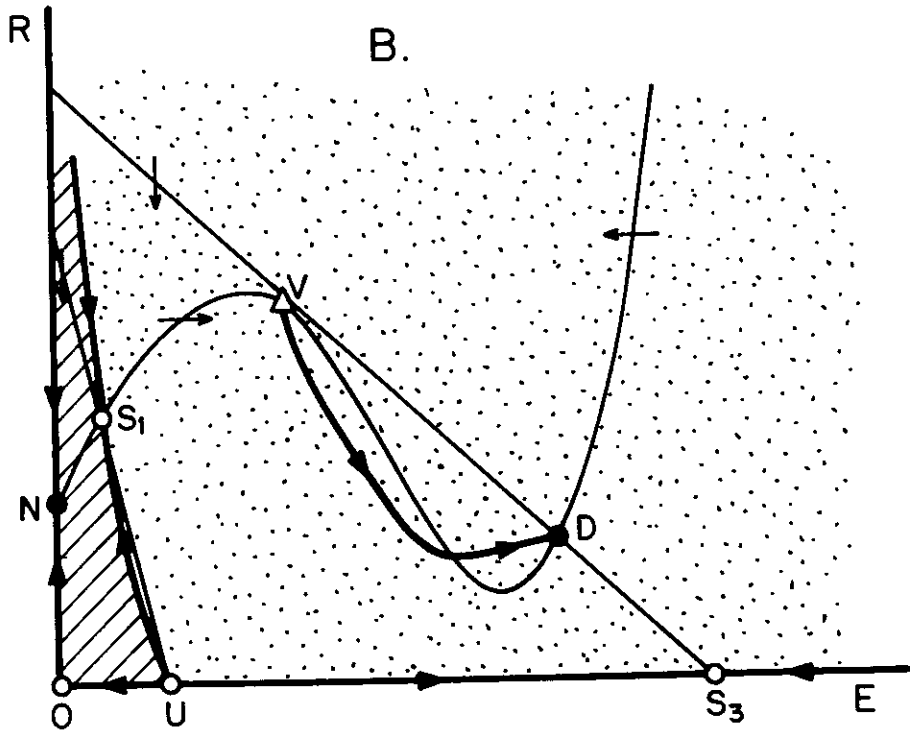

Fig. 17

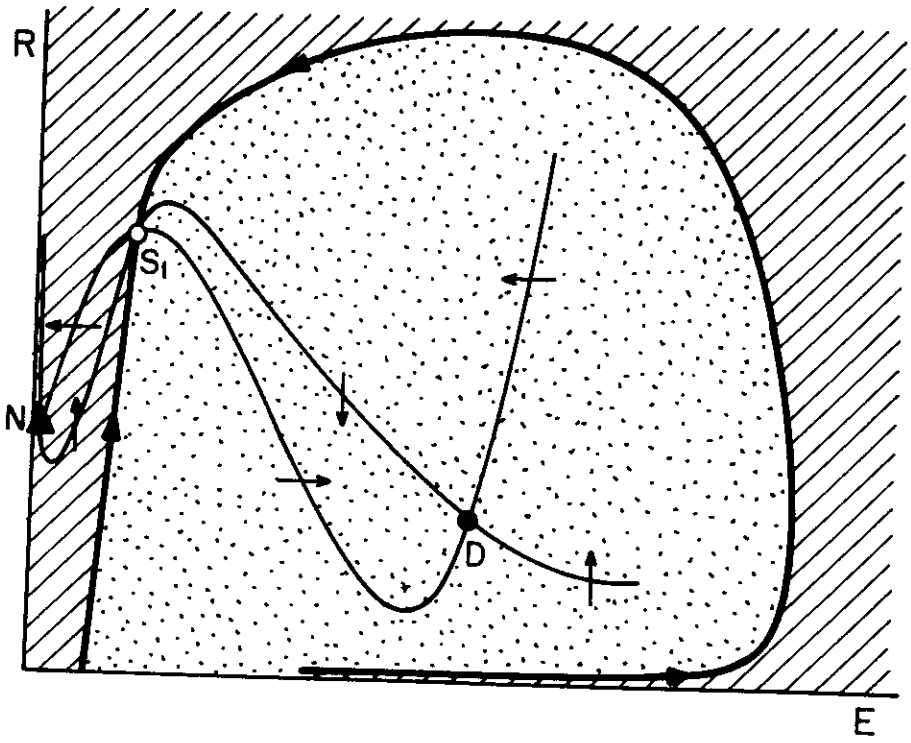

Fig. 18

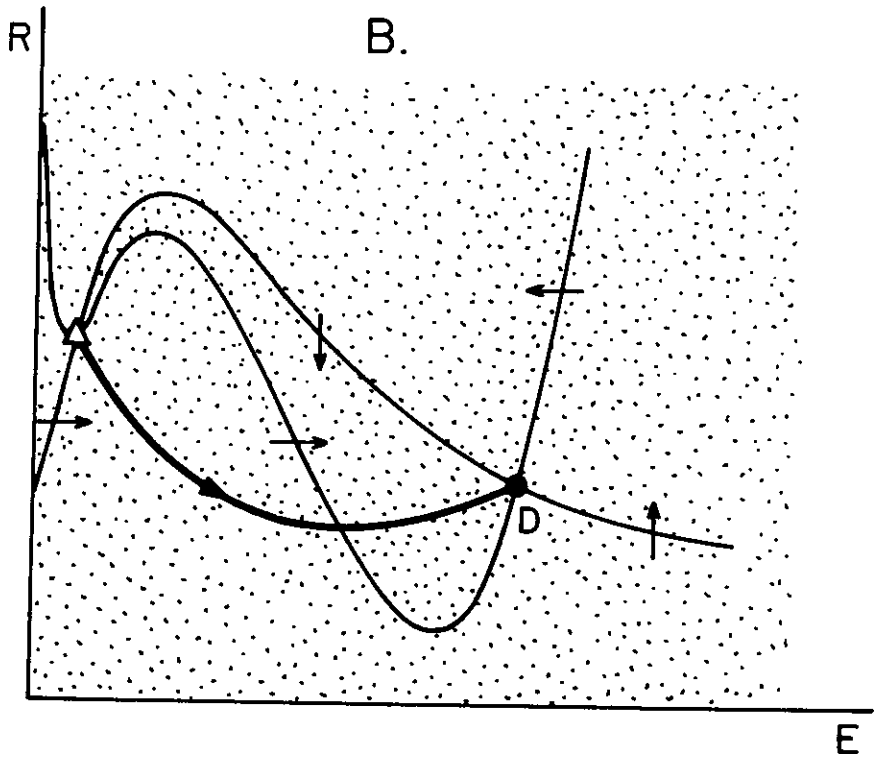

Fig. 18

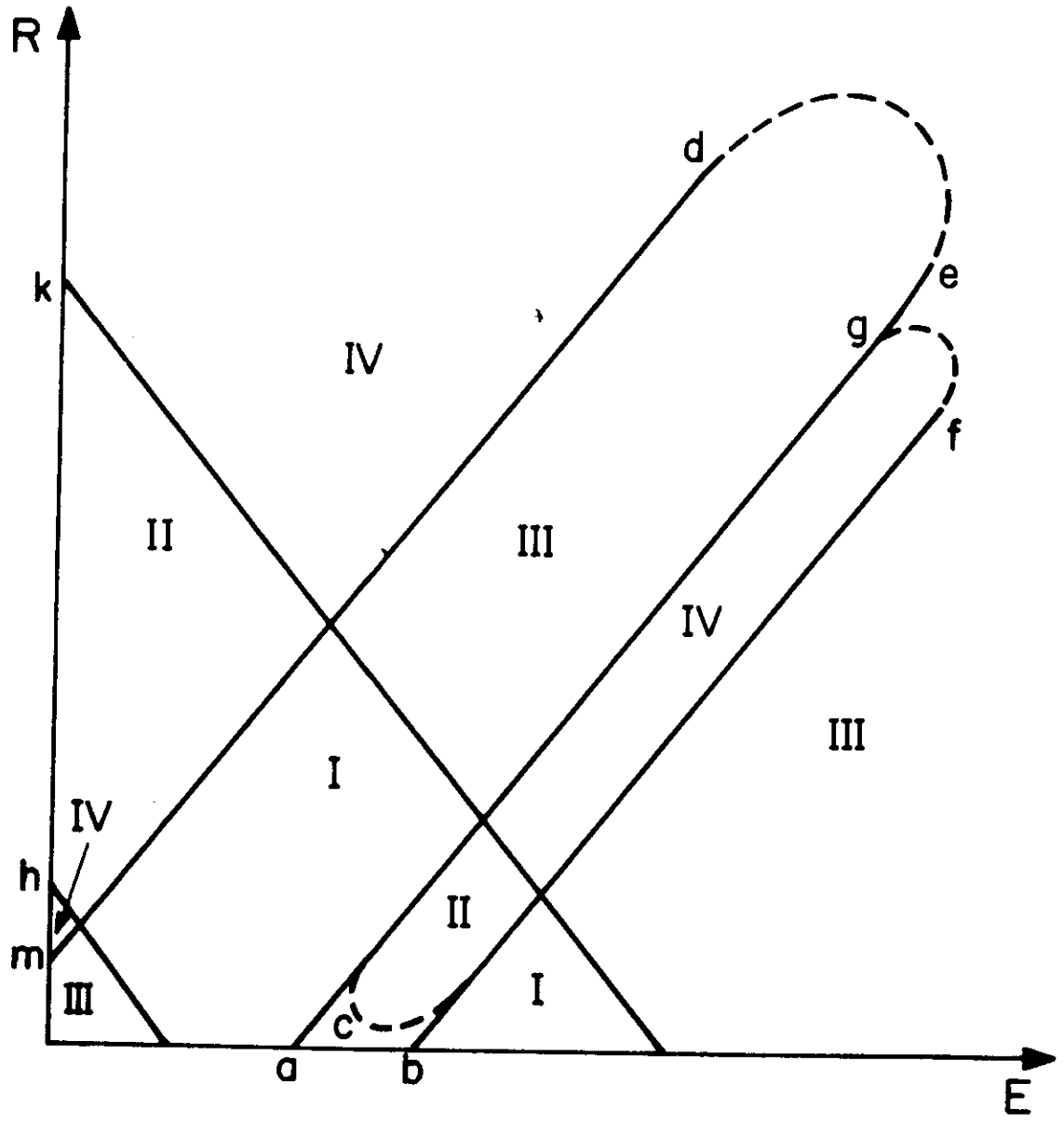

Fig. 19

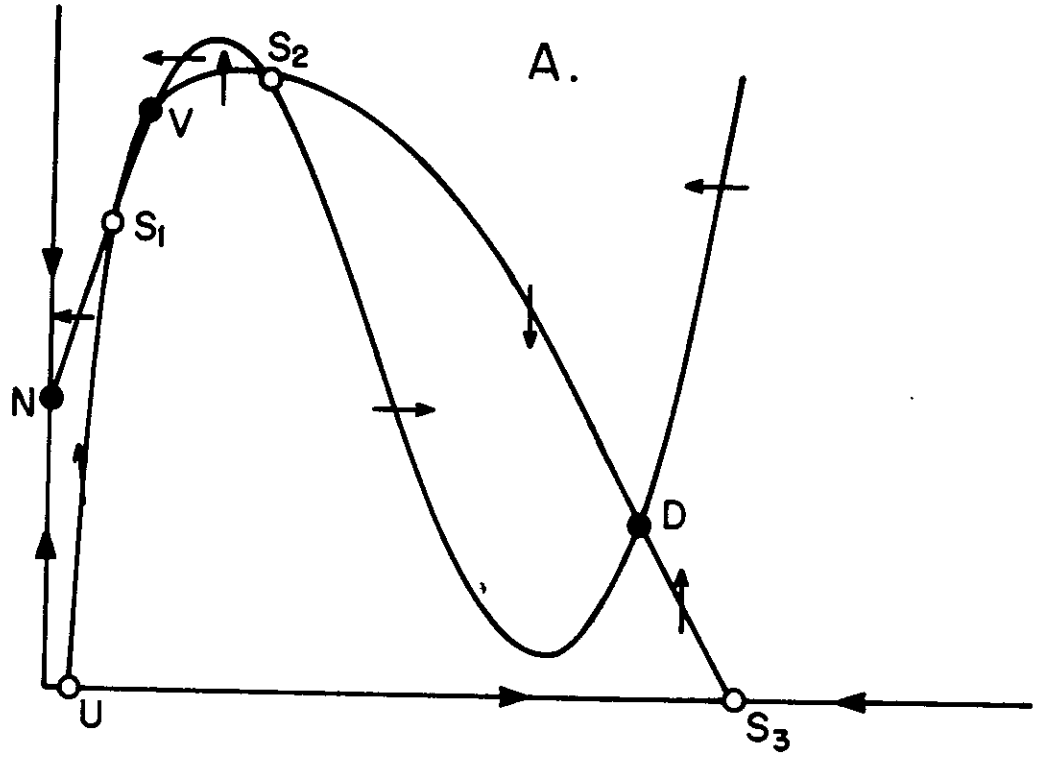

Fig. 20

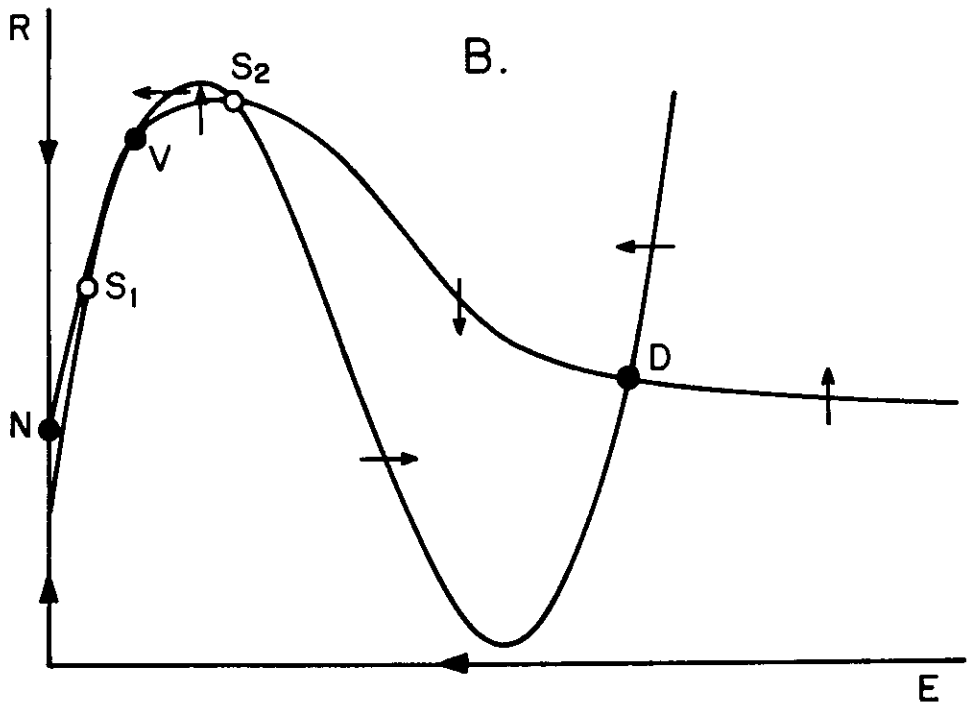

Fig. 20